Peter Prandner, BSc

Continuous cross-coupling reactions using a granulated heterogeneous palladium catalyst

MASTERARBEIT

zur Erlangung des akademischen Grades

Master of Science

Masterstudium Verfahrenstechnik

eingereicht an der

Technischen Universität Graz

Betreuerin

Ass. Prof. Dipl.-Ing. Dr.techn. Heidrun Gruber-Wölfler

Institute of Process and Particle Engineering

Graz, April 2018

EIDESSTATTLICHE ERKLÄRUNG

Ich erkläre an Eides statt, dass ich die vorliegende Arbeit selbstständig verfasst, andere als die angegebenen Quellen/Hilfsmittel nicht benutzt, und die den benutzten Quellen wörtlich und inhaltlich entnommenen Stellen als solche kenntlich gemacht habe. Das in TUGRAZonline hochgeladene Textdokument ist mit der vorliegenden Masterarbeit identisch.

Datum

Unterschrift

Abstract

The goal of this work is to develop a way to enlarge the particle size of a given heterogeneous palladium catalyst and to test it for Suzuki-Miyaura and Heck reactions. This enlargement of the catalyst is necessary for easy handling and to simplify the removal of the catalyst from the product. This is particularly important for integrated processes, e.g. synthesis directly coupled to purification.

After a screening of different methods for particle enlargement, especially agglomeration, coating, sintering or pressing and milling, a suitable method was chosen. In this case, the decision was made for pressing and milling to generate a palladium catalyst granulate with an average particle size of 1 mm. For this purpose, the catalyst was mixed with a binder (calcium sulphate) to improve the stability of the pressed tablets and to achieve good milling behaviours.

In the next step, the performance of the granulated catalyst was tested in different batch experiments for given Suzuki-Miyaura and Heck reactions. For this purpose, the stock solution of the reactions was kept constant and the amount of granulate was varied.

Finally, the granulate was tested in a continuous process, which was realized with the so-called plug&play reactor. This modular reactor makes it possible to keep the reaction temperature constant and to vary the mass of the catalyst by varying the number of columns in the reactor. Furthermore, it was possible to vary the volumetric flow, to increase the residence time and thereby the conversion of the substrates.

Kurzfassung

Ziel dieser Arbeit ist es, eine Methode zu entwickeln, um die Partikel eines gegebenen heterogenen Palladiumkatalysators zu vergrößern und für Suzuki-Miyaura und Heck Reaktionen zu testen. Diese Partikelvergrößerungen sind notwendig um den Katalysator einfacher zu händeln und die Abtrennung vom Produkt zu vereinfachen. Speziell für Aufarbeitungsprozesse bei kontinuierlichen integrierten Prozessen ist dies von Bedeutung.

Nach einem Screening von verschiedenen Methoden für Partikelvergrößerungen, insbesondere Agglomeration, Beschichten oder Pressen und Mahlen, wurde eine passende Methode gewählt. In diesem Fall fiel die Entscheidung für Pressen und Mahlen, um ein Palladium-Katalysator Granulat von einer durchschnittlichen Partikelgröße von 1 mm herzustellen. Dafür wurde der Palladium-Katalysator mit einem Bindemittel (Kalziumsulfat) versehen, um die Stabilität der gepressten Tabletten zu erhöhen und gute Mahleigenschaften zu erhalten.

Im nächsten Schritt wurde die Leistungsfähigkeit des granulierten Katalysators in verschiedenen Batch-Versuchen für gegebene Suzuki-Miyaura und Heck Reaktionen getestet. Dafür wurde die Ausgangslösung der Reaktionen konstant gehalten und die Masse an Granulat variiert.

Schließlich wurde der granulierte Katalysator in einem kontinuierlichen Prozess getestet. Dies wurde mit dem so genannten Plug&Play Reaktor realisiert. Dieser modulare Reaktor bietet die Möglichkeit die Reaktionstemperatur auf einem konstanten Level zu halten und die Masse an Granulat zu variieren indem man die Anzahl der Säulen im Reaktor verändert. Darüber hinaus kann der Volumenstrom verändert werden, um die Verweilzeit zu erhöhen und so den Umsatz vom Substrat zu steigern.

Acknowledgment

I owe my sincerest gratitude to everyone who supported me while writing this thesis.

First of all, I would like to thank my supervisor Heidrun Gruber-Wölfler and Bianca Grabner for their professional guidance and support.

Of course I want to thank the laboratory personal for the great support during all the time of my master thesis in the laboratory.

Last but not least, I want to thank my family and friends who supported me throughout my years of study.

Content

List of Figures:

List of Schemes:

List of Tables:

List of Abbreviations:

API	active pharmaceutical ingredient
RTD	residence time distribution
HPLC	high performance liquid chromatography
GC	gas chromatography
BET	Brunauer-Emmet-Teller (surface analysis)
TON	turn over number
TOF	turn over frequency
$E_{(t)}$	E-function (residence time distribution)
$F_{(t)}$	F-function (cumulative density function)
c_i , C	concentration
t	time
t_m , $\bar{t}$	mean residence time
Θ	dimensionless time variable
σ^2	variance
σ_Θ	variance, referred to dimensionless time variable
Bo	Bodenstein number
$\bar{u}$	mean internal velocity in the column
L	length of the column
D_{ax}	axial diffusion coefficient
φ_p	particle volume fraction
V_{cat}	volume of the catalyst
V_r	volume of the column
V_l	volume of the liquid
ε	bed porosity
Y_p	reactive catalyst volume per fluid volume

1 Introduction

During the last few decades, palladium catalyzed cross-coupling reactions such as Heck, Suzuki-Miyaura, Negishi, Sonogashira reactions, *etc.* made it possible to develop many valuable synthetic routes [1]. To create new C-C bonds, these reactions are normally performed with homogeneous catalysts. It is difficult to remove or separate the homogeneous palladium catalysts from the products, but it is unavoidable for wide applications at large scale due to the high cost of palladium catalysts coupled with toxic effects. For example, in the production of fine chemicals or active pharmaceutical ingredients (APIs), it is necessary to avoid contamination of the product [2]. To solve this problem, the palladium catalysts can be immobilized, which is helpful especially for continuous multistep API synthesis or end-to-end manufacturing, to simplify the downstream process [3].

The reaction mixture in a typical heterogeneous batch reaction, containing the immobilized catalyst, is stirred under optimized conditions to reach the desired transformation. Afterwards, the catalyst can be easily removed by filtration. This makes it possible to reuse the catalyst and most of the metal remains on the support, so the contamination of the product is kept at a minimum. In a continuous flow process, the catalyst is typically placed in a packed-bed reactor, so the reaction mixture can be pumped through the bed. Therefore, the reaction and separation of the catalyst take place simultaneously. This kind of reaction setup avoids an additional separation/filtration step for the catalyst and simplifies the re-use and recycling of the catalyst [4].

In this work, the heterogeneous palladium catalyst $Sn_{0.99}Pd_{0.01}O_{2-\delta}$ was used for the Suzuki-Miyaura and the Heck reaction. Reported by Georg Lichtenegger et al. [5] this catalyst has the best performance according to conversion and yield of the tested catalysts. The catalyst is enlarged to a particle size of about 1 mm in diameter. This way, the separation in the continuous process is much easier and the pressure loss in the packed bed reactor can also be reduced, compared to using the original fine particle size in the reactor. Several batch-experiments were conducted in order characterize the catalyst granulate. Afterwards, the catalyst was tested in the continuous flow, the so called plug & play reactor.

Every Suzuki-Miyaura reaction was carried out using 4-bromotoluene and phenylboronic acid as substrates and varying amounts of the catalyst ($Sn_{0.99}Pd_{0.01}O_{2-\delta}$). This coupling reaction leads to 4-methylbiphenyl, as depicted in Scheme 1 [5].

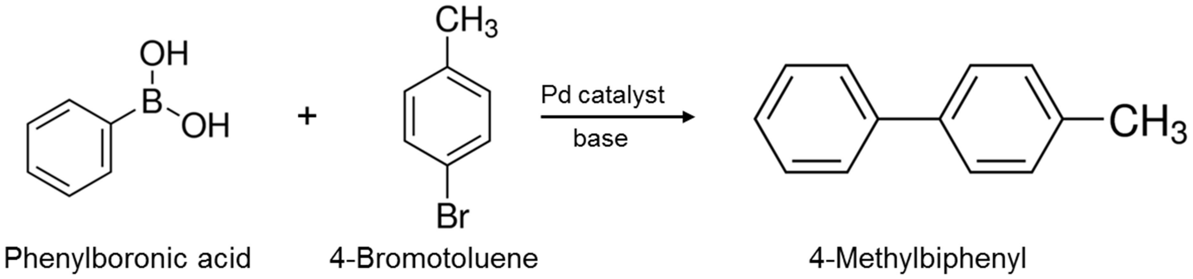

Scheme 1: Suzuki-coupling between phenylboronic acid and 4-bromotoluene

The Heck experiments were carried out using iodobenzene and 3-butene-2-ol as substrates and varying the amount of the catalyst ($Sn_{0.99}Pd_{0.01}O_{2-\delta}$). This coupling reaction leads to 4-phenyl-but-3en-2ol, as depicted in Scheme 2.

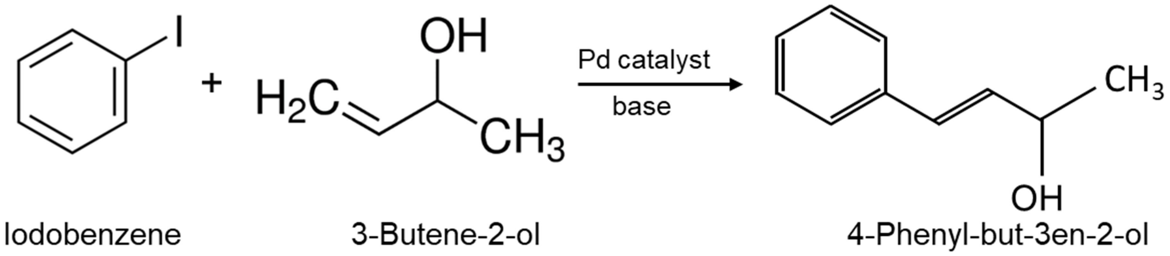

Scheme 2: Heck-coupling between iodobenzene and 3-butene-2-ol

2 Theoretical Background

In order to increase the rate, efficiency, and selectivity of the desired chemical reactions, catalysts are used. Heterogeneous catalysts typically consist of an active material immobilized on a porous support. Depending on the application, these support or catalyst powders are often agglomerated into various millimetric shapes in order to improve handling [6].

2.1 Granulation

Two common particle size enlargement processes are granulation and tabletting to combine small particles or multiple powder ingredients into a structured particle assembly. These processes are commonly used to produce pharmaceuticals, catalyst carriers or detergents, to name a few. In order to meet the product specifications granules of sufficient size, shape, composition, and a suitable internal structure are required. Goals that can be achieved by granulation and/or compaction are [7]:

- Ensuring all powdered ingredients are uniformly mixed in view of strict composition
- An increase in bulk density
- The production of compacts that have a high specific surface area and a well-designed pore structure
- The production of pellets that cause little pressure drop in fixed beds

The two key types of granulation processes are wet and dry granulation. For wet granulation, a liquid is used to agglomerate the powder. During dry granulation or roller compaction, the powders are compressed together to form granules [6].

Granulation Mechanism

The mechanism for the growth of particles in wet granulation is a three-part process, consisting of the process below (Figure 1).

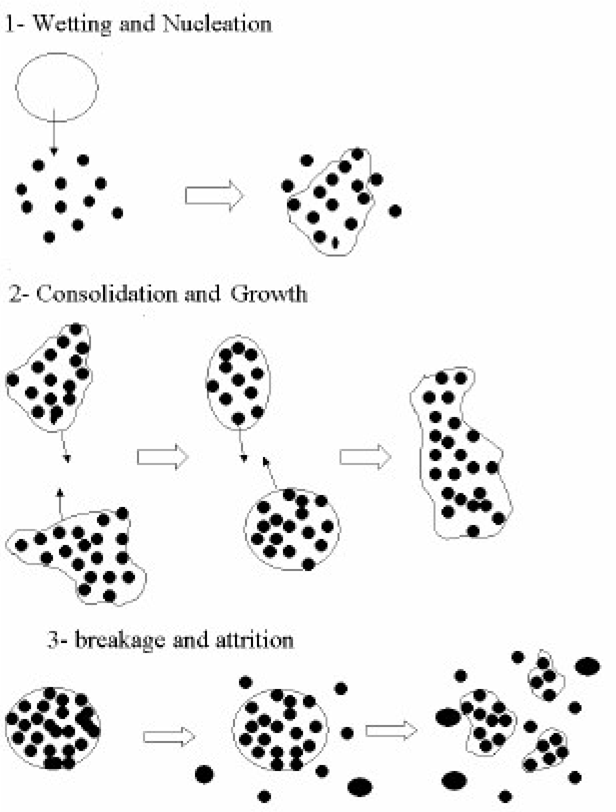

Figure 1: Mechanism of the growth of particles [8]

Nucleation describes the contact of the initial dry powder with the binder and the subsequent formation of the nucleus. The nucleation is droplet-controlled. Every droplet forms a single nucleus due to mechanical dispersion, where clusters are formed by multiple droplets coalescing. Under shear they are broken up into multiple nucleates.

Granule growth describes the collision of two larger particles as a result of coalescence or agglomeration. It is affected by properties of particle size, binder, bulk powder and mechanical properties.

Breakage and attrition act to decrease the size of the granule. It influences and even controls the final size distribution up to the limitation of the maximum granule size [8].

Granulation Equipment

Wet granulation equipment has two common aspects: mixing and turning over the powder and introducing the liquid binder to the powder mass. The granulator design and operation have a strong effect on granule properties such as size distribution or porosity [6]. Three common methods that are used for granulation in the industry are drum granulators, mixer granulators, pressing and milling.

Drum Granulators

Drum granulation is commonly used to manufacture spherical granules and is a well-established unit operation [9, 10]. In general, large granules in the range of 1-10 mm are produced by spraying the binder fluid on the incoming dry powder at the entry of the drum [6].

Mixer Granulators

Mixer granulators agitate and mix powders by using rotating impellers or paddles. They can be classified as high shear (most common) or low shear mixers, depending on the impeller rotation speed. Additionally, they often have a small high-speed rotating impeller, called "chopper" to break up oversized granules [6]. Generally, a high-shear mixer produces granules in a range between 200 and 1000 µm [11].

Pressing and Milling

The compaction force of pressing that allows the powder bed to convert includes different mechanisms. Tableting generally consists of two phases. In the first phase, compression pushes the particles closer together. During the second phase, the packing volume is no longer reduced but deformed by brittle fracture or by plastic flow [12].

The compression stage will set up the process of compact formation and is related to a number of factors, for example particle size and shape with surface area and surface roughness. Also the physical form of the material, if it is amorphous or crystalline affects the compression [13].

During the second stage of the compaction, the surface is changed because of fracture and flow which is effected by the porosity of the material. These changes are also often correlated to tablet strength [14].

Rumpf [15] describes five types of bonding mechanisms:

- Solid bridges (crystallization of amorphous solids, sintering chemical reactions)
- Movable liquids (related to surface tension forces)
- Non-freely movable binders (wet granulation processing)
- Attraction between solid particles
- Mechanical interlocking

Normally, solid bridge formation, intermolecular forces and mechanical interlocking are the dominant mechanisms [16].

Afterwards, the pressed tablets are milled to achieve the required particle size distribution for the catalyst granulate. Generally, milling can be divided into dry and wet milling. In this case, the decision was made to use dry roller milling, as it is used in peppermills. This grinding process reduces the tablets to a smaller particle size by pressure and shear [17]. Especially for the catalyst, it is necessary to have small particles because this results in a higher specific surface area which means that the reactions run faster.

2.2 Coupling Reactions

"Coupling reactions involve the formation of a C-C bond and are simple and straightforward. Industrially, coupling reactions form a part of a large number of multistep synthesis processes. These reactions are highly selective and give high yields because they involve specific reactions between carbon centered anions with polar compounds such as esters and ketone, and metal halides. There are two types of couplings [18]:

- Cross-coupling: This involves two different species forming a C-C bond such as bromobenzene and vinyl chloride to give styrene.
- Homo-coupling: This involves the formation of a C-C bond between two identical partners such as the conversion of iodobenzene to biphenyl. "

What plays an important part in the reactivity and selectivity of the reaction is the choice of the ligand and the catalyst. With metal catalysts such as palladium, nickel or cobalt, coupling reactions have increased manifold. Palladium as a catalyst has been used very often because it gives a very high activity allowing for a higher conversion at moderate conditions compared to other metal counterparts [19]. In this thesis, two coupling reactions, the Heck and Suzuki-Miyaura reaction are going to be used.

2.2.2 Heck coupling reaction

Heck coupling reactions implicate a bond formation between aryl halides and alkenes in the presence of a base. An efficient catalyst system for this purpose is palladium, which is in general an important catalyst in the C-C bond formation in synthetic organic chemistry, as shown in Scheme 3.

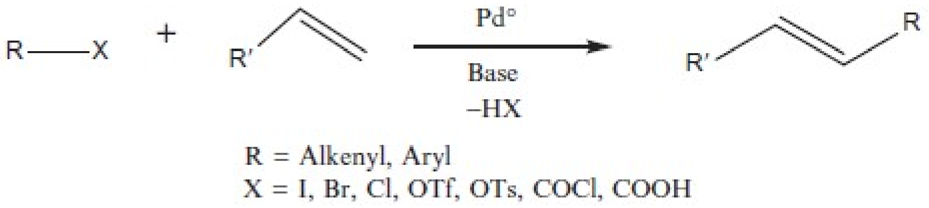

Scheme 3: Heck-coupling with palladium catalyst for olefins and alkyl halides

Scheme 4 illustrates the mechanism of the Heck coupling.

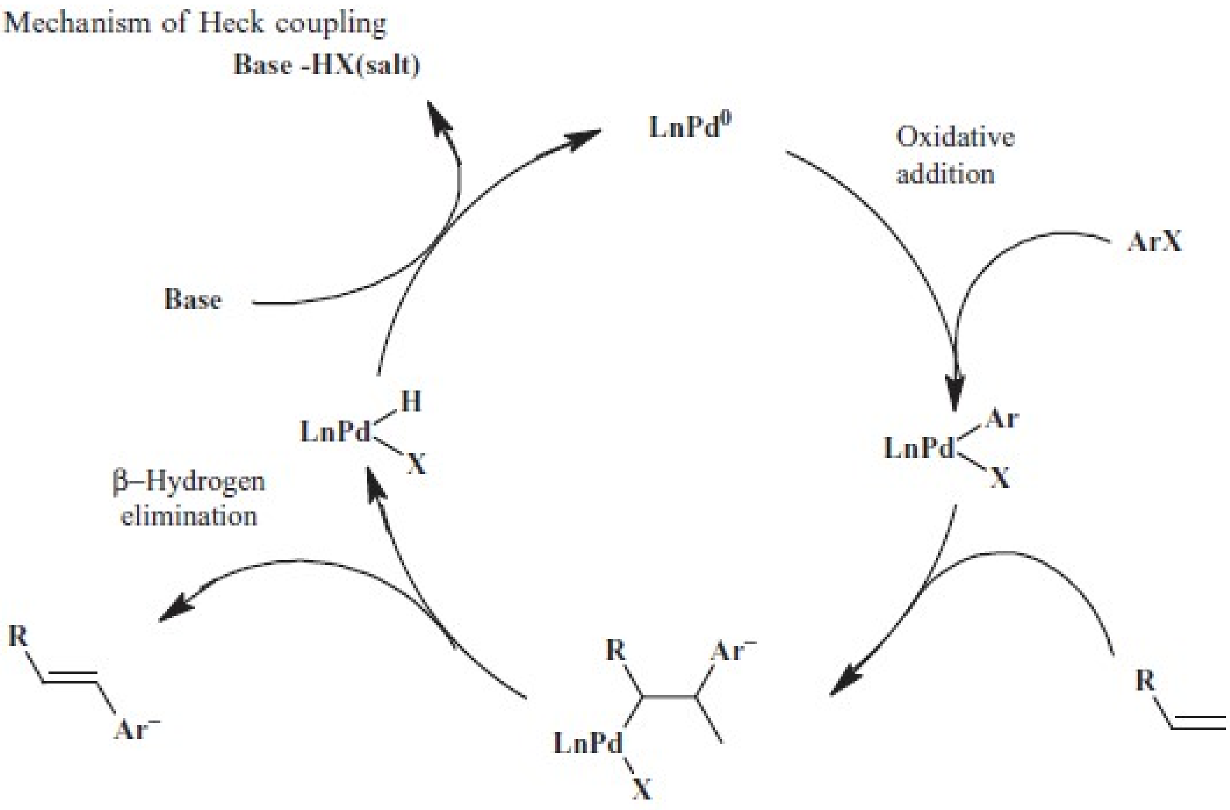

Scheme 4: Catalytic cycle of the Heck reaction [22, 23]

Step 1: Oxidative addition

The electron donating groups for example phosphine ligands can activate the Pd(0) catalyst such that the R-X bond can be easily broken along with the formation of Pd-R and Pd-X bond. [35]

Step 2: Migration insertion

Before migratory insertion of the olefin to the palladium-R bond, the olefin must first associate onto the palladium complex, which requires the dissociation of the existing ligands.

Migration insertion of the Pd-R bond can control the stereo-selectivity and regio-selectivity of Heck reactions. For a neutral palladium complex, the region-selectivity is governed by steric, which means nucleophilic attack happens on the less hindered side of the alkene [37].

Step 3: β-Hydride Elimination

β-Hydride elimination results in the Heck reaction product, which is a new substituted alkene. In this step, the palladium and the hydride attached to it must be *syn*-coplanar for the initiation of elimination [36].

Step 4: Regeneration of palladium catalyst

The addition of base is necessary to reduce the L_nPdHX complex back to the starting $L_nPd(0)$ to close the catalytic cycle.

2.2.1 Suzuki-Miyaura coupling reaction

This coupling reaction is defined as a process for the formation of the C-C bond between an organic halide and an organoboron compound. In the reaction mechanism the organometallic compound acts as a nucleophile and the organic halide acts as an electrophile. The Suzuki-Miyaura reaction was first metioned in [20] and became an important method for aryl-aryl bond formation. Its mild reaction conditions and ability to synthesize highly functionalized molecules and ease of availability of boronic acids is a big advantage of the process. The reaction may proceed in water because the phenyl boronic acid is soluble in water. In Scheme 5, the Suzuki-coupling with a palladium catalyst is displayed.

Scheme 5: Suzuki-coupling with palladium catalyst [21]

As shown in Scheme 6, the choice of the solvent, base, ligand and metal are important for influencing the transmetallation, the reductive elimination steps, and the oxidative addition [21].

Step 1: Oxidative addition

Oxidative addition is known to proceed with retention of stereochemistry with vinyl halides and with inversion with allylic or benzylic halides. This gives a *cis* complex that rapidly isomerizes to its *trans* isomer [38].

Step 2: Transmetallation

Organoboron compounds are highly covalent in character and do not undergo transmetallation readily in absence of base [38].

Step 3: Reductive Elimination

Isomerization to the *cis* complex is required before reductive elimination can occur [38].

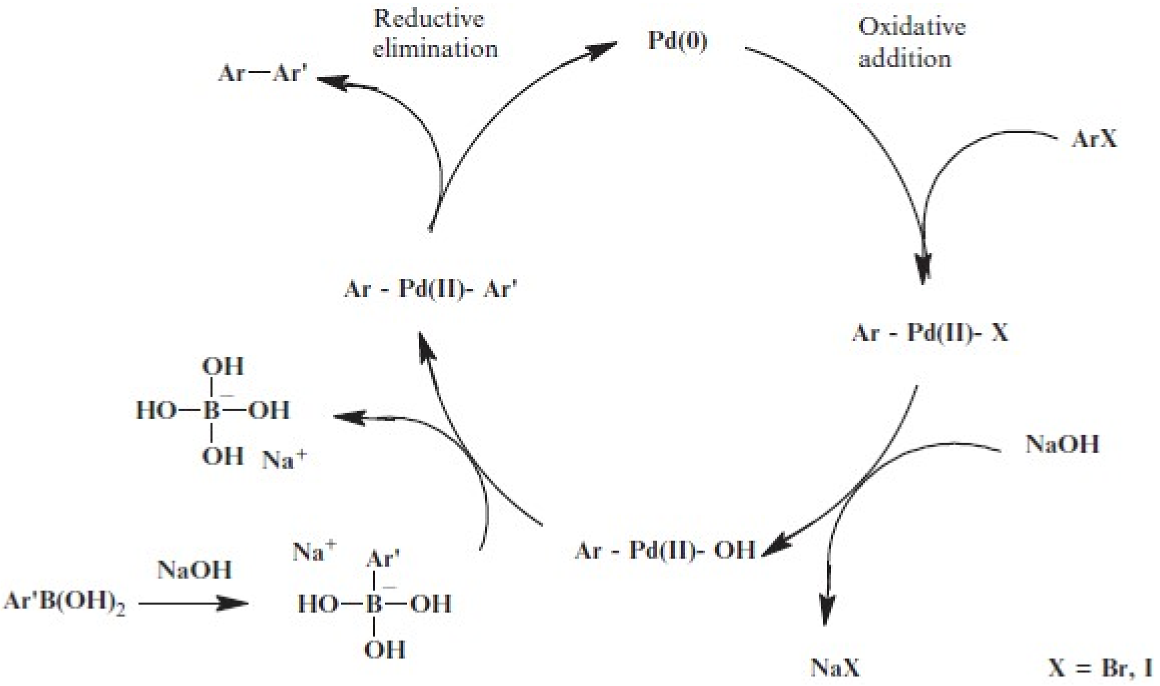

Scheme 6: Mechanism of the Suzuki-coupling [21]

In this thesis Suzuki-Miyaura coupling reactions are also carried out in a continuous flow process, which are described in the following.

2.3 Continuous Flow

Common industrial processes, especially petrochemicals, are traditionally carried out in continuous flow systems. Contrary, most fine chemicals and pharmaceuticals were produced in batch processes. Recently, for production of fine chemicals and pharmaceuticals, the continuous flow synthesis became more and more popular, not only to improve the selectivity, safety, and sustainability, but also the efficiency of developing new drugs and functional materials of chemical production [24].

Advantages of continuous flow synthesis

Continuous flow synthesis leads to several advantages compared to continuous flow synthesis. It is very time-efficient for screening a large number of compounds for synthesising. However, to automate a chemical reaction, continuous flow processes are more suitable. [39] Further advantages of continuous flow synthesis are: At the inlet of the reactor, starting material and reagents are fed by pumping. Inside the reactor the solid catalyst is provided. Compared to batch synthesis, there are several advantages of continuous flow synthesis [26, 27]:

- Fast mixing: (for microreactors) chemical reactions are the results of combining two or more substances, which is why it is very important that the substances are homogeneous [24].

- Mass transfer between phases: (for microreactors) In flow reactors, especially in micro rectors make phase boundary reactions such as liquid/liquid reactions are more efficient [28].
- Temperature control of the reaction
- Residence time control: residence increases with the length of the channel and decreases with the flow velocity (for plug flow reactors)
- Safe handling of hazardous reagents or intermediates, especially for microreactors [24].

2.3.1 Residence time distribution (RTD)

To diagnose flow behaviour within a wide range of flow systems, residence time distribution (RTD) measurements are very effective. RTD analysis of a controlled tracer addition into a system can reveal flow distribution characteristics such as transit times, short circuiting, re-circulation zones, and dead zones. RDT methods may also be used to develop and validate flow models, and can be applied to field and lab scale systems [40].

Every dynamic signal with a sufficient temporal resolution, which can be realized at the inlet and detected at the outlet, can be used for determining the residence time distribution of a system. The step function or pulse function (see Figure 2) are the most common methods for realizing the measurements. A preference of the step function is that all information of the dynamic process is included. This leads to tightly packed process information, and as a consequence, inaccurate measurements mean that details can be lost. Easier to interpret is the pulse function. When this function is used, a model could be fitted easier. To reproduce an impulse function exactly is impossible but it can be approximated through a fast addition of the tracer. [31]

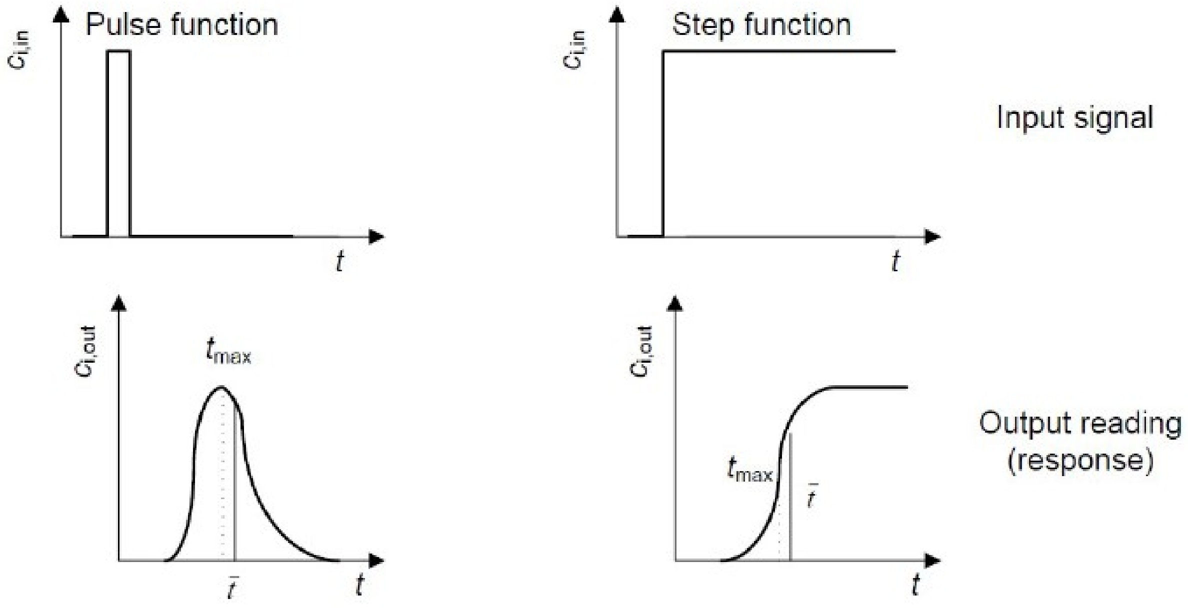

Figure 2: Input and output signal of the tracer in a plug flow reactor [25]

Visualizing a function at the process inlet, either the concentration of an already used component can be varied or a tracer material can be added extra. A step- function was chosen for this work, because the concentration of the inlet was varied and the samples were taken continuously every two minutes at the outlet.

To ensure a successful implementation in practice, the following conditions have to be made:

- The quantity (signal) has to be easily measured
- Changes must not cause any disturbances of the flow conditions

The residence time distribution can be described as a population density function (E-function) and a cumulative density function (F-function) (see Figure 3) [29].

The residence time distribution (E- function) is defined as the material portion at the outlet of a system at a certain time [30]:

$$E_{(t)} = \frac{C_{(t)}}{\int_0^\infty c dt} \sim \frac{C_{(t)}}{\sum_0^\infty c\Delta \mathrm{t}} \qquad (1)$$

The F-function can be calculated from the E-function. It represents the accumulation of the tracer at the exit with the residence time t [30]:

$$F_{(t)} = \int_0^t E_{(t)}\, dt \cong \frac{\sum_0^t c\Delta t}{\sum_0^\infty c\Delta t} \qquad (2)$$

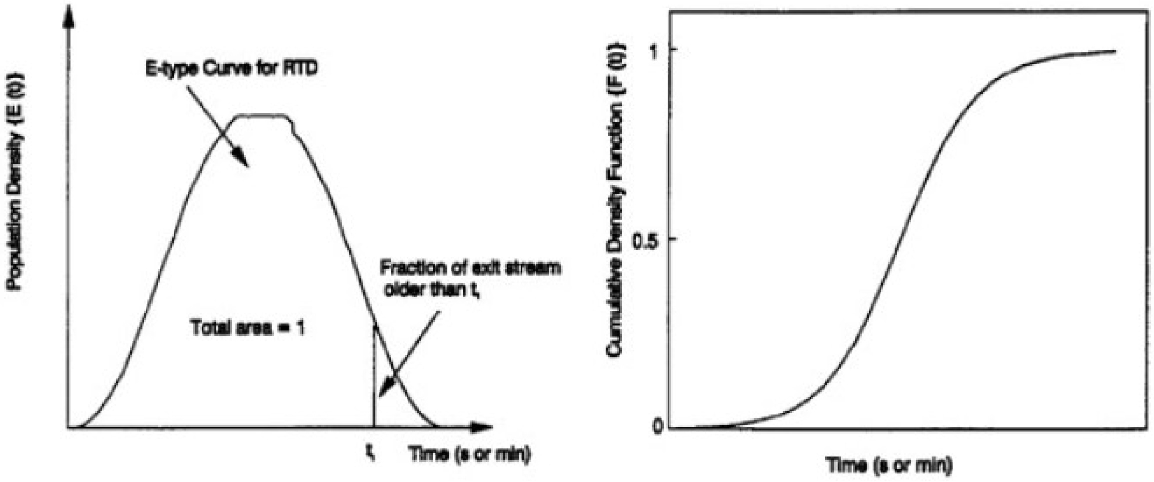

Figure 3: Left: E-function, right: F-function [41]

The mean residence time can be calculated as follows [30]:

$$t_m = \int tE_{(t)}\, dt \sim \frac{\sum_0^\infty tc\Delta t}{\sum_0^\infty c\Delta t} \tag{3}$$

For comparative purposes, a dimensionless time variable is often useful, which is the ratio of the fluid residence time to that of the mean residence time of the carrier fluid [31].

$$\theta = \frac{t}{t_m} \tag{4}$$

The width of the distribution, characterized by the variance can be described as follows:

$$\sigma^2 = \sum_0^\infty (t - t_m)^2 E_{(t)} \tag{5}$$

The axial dispersion coefficient describes the degree of axial back mixing in the flow, which affects the conversion of chemical reactions. The dimensionless Bodenstein number Bo is the ratio of convective mass transfer to axial dispersion.

$$Bo = \frac{\bar{u} * L}{D_{ax}} \tag{6}$$

A high Bodenstein number is equivalent to a flow with low axial back-mixing, which means the flow regime in the reactor is a plug-flow. While a small Bodenstein number is equivalent to a flow with a high degree of axial back mixing, which leads to a more turbulent flow.

For Bodenstein numbers Bo > 100, the solution differential mass transfer equation at dimensionless RTD is:

$$\sigma_\theta^2 = \frac{{\sigma_t}^2}{\bar{t}^2} = \frac{2}{Bo} \tag{7}$$

For high dispersion (Bo < 100), the Bodenstein number can be calculated at a dimensionless RTD [25]:

$$Bo = \frac{1}{\sigma_\theta^2} + \sqrt{\left(\frac{1}{\sigma_\theta^2}\right)^2 + \frac{3}{\sigma_\theta^2}} \tag{8}$$

2.3.2 Key parameters for a packed bed reactor

In order to characterize the packed bed reactor, some key parameters are necessary. Therefore, the assumption that granulate consists of spherical particles was made. The specific surface area and particle size distribution were measured. Furthermore, the particle volume fraction, the bed porosity, and the reactive catalyst volume per fluid volume could be calculated [33].

Particle volume fraction

$$\varphi_p = \frac{V_{cat}}{V_r} = \frac{V_{cat}}{V_l + V_{cat}} \tag{9}$$

Bed porosity

$$\varepsilon = \frac{V_l}{V_r} = 1 - \varphi_p \tag{10}$$

Reactive catalyst volume per fluid volume

$$Y_p = \frac{\varphi_p}{1 - \varphi_p} \tag{11}$$

3 Results

For the granulation, four different methods were carried out. These methods are agglomeration, coating, sintering, as well as pressing and milling.

The chosen method for agglomeration was high-shear agglomeration. Therefore, three different binder (potassium carbonate, dextrin, and alginic acid sodium salt) were investigated. This compounds were premixed under dry conditions and under high-shearing water was added for agglomeration.

Coating was done by rolling pellets (gravel pellets, glass pellets, and alumina oxide pellets) in a slurry of catalyst and binders (binder: potassium carbonate, dextrin, and alginic acid sodium salt). Afterwards, the coated pellets were dried in a compartment dryer.

For sintering, the slurry of the crude catalyst was added with pellets to fix it on with a thermal treatment during production on a temperature of 350°C.

Pressing and milling was done by pressing a mixture of catalyst and binder (calcium sulphate) to tablets and milling them to the demanded particle size. For this, an amount of 150 mg with different compositions of catalyst and binder were pressed in two different dies with 8 mm and 10 mm in diameter.

More details to the different processes are given in the following.

3.1 Granulation

Agglomeration:

For agglomeration, the agglomerated particles with the different binders were investigated with a microscope (Leica, Type: DM4000M) to analyse the structure of the particles. In the first step, the potassium carbonate was used as binder (see Figure 4). Here, it can be seen that potassium carbonate is not suitable as a binder because it is too hydrophilic and adsorbs water from air. Dextrin is much better as a binder as shown in Figure 5, but the particles are mechanically not very stable and crumble very easily. Furthermore, it is not stable in the solvent. Finally, alginic acid sodium salt was investigated as a binder (see Figure 6), but it also crumbles very easily and it is not stable in the solvent.

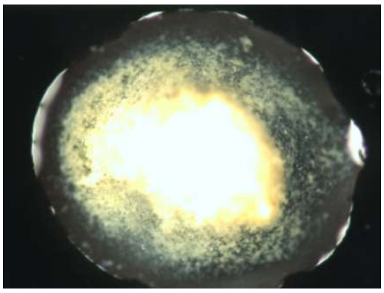

Figure 4: Catalyst particles with potassium Carbonate as binder

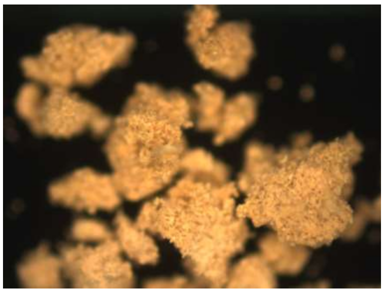

Figure 5: Catalyst particles with dextrin as binder

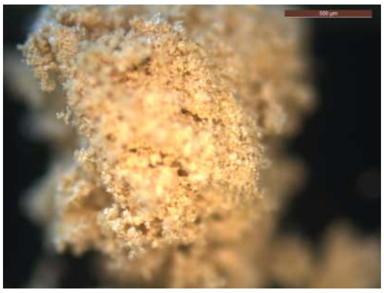

Figure 6: Catalyst particles with alginic acid sodium salt as binder

Coating:

At first, it was investigated whether coating with the drum granulator works. The big disadvantage of this is that the glass pellets with a diameter of 1.5 to 1.85 mm for coating stack on the inner layer of the drum granulator when they get wet and, as a result, the effect of rolling over the mixture of catalyst and binder gets lost. In Figure 7 it can be seen that the coating generally works, but the layer is very inhomogeneous.

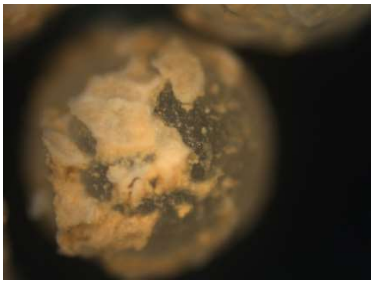

Figure 7: Coated glass pellets

In the next step, the pellets were wetted with the binder and rolled in the dry catalyst to fix them to the pellets. Figure 8 shows the coated glass pellets. What is problematic, is that they have a very smooth surface, which is why the catalyst does not stick to the surface very well and can be removed rather easily. Next, gravel pellets were tested, because their surface is rougher than that of glass pellets (see Figure 9). However, the binders that were used, potassium carbonate, dextrin and alginic acid sodium salt, also did not fix the catalyst very well to the surface. Figure 10 shows the coated gravel.

Figure 8: Glass pellets rolled in catalyst

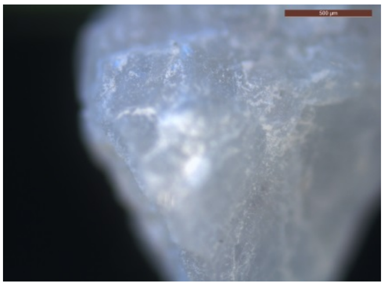

Figure 9: Neutral gravel

Figure 10: Coated gravel

In the last step, alumina oxide pellets were used for coating and calcium sulphate was used as a binder. The coating stuck very well to the surface, but the coating was very thick and the pellets reached a size of about 10 mm, which was too big (see Figure 11). Therefore, the active surface is very small compared to the mass of the catalyst.

Figure 11: Coated alumina oxide pellets

Sintering:

The gravel that was used to immobilize the catalyst on seemed to work very well (Figure 12), but the size of the catalyst is too big to adhere in the pores. By this mode of operation, the catalyst is rubbed off the gravel and gets into the solvent.

Figure 12: Sintered catalyst on gravel

Pressing and Milling:

For pressing, calcium sulphate was used as a binder with different amounts of the binder and the catalyst. In addition, the pressure for tableting was varied between 2.5 to 5 tons to find the optimum hardness for the tablets. In connection, the tablets were milled down to a size of 1 mm. The first experiments were carried out with a die of 8 mm in diameter. This die allows a maximum pressure of 5 tons. 150 mg of pure catalyst were filled in the die and pressed, and afterwards they had a height of 1.1mm (Figure 13). Under the microscope the homogeneity of the mixture on the surface of the tablet was checked with an amount of catalyst to binder of 1:1, as can be seen in Figure 14. The dark area is catalyst, the white one represents the binder.

Figure 13: Tablet with die 8 mm

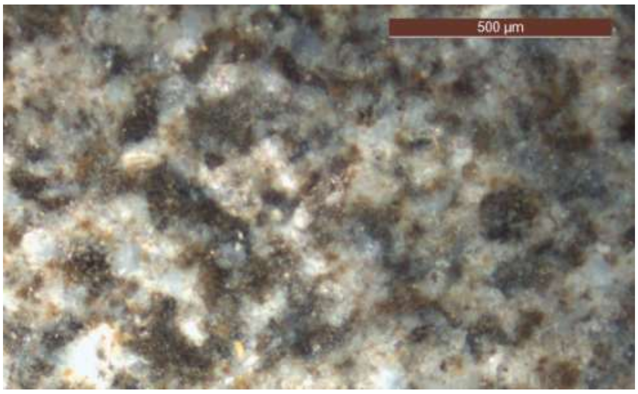

Figure 14: Microscopic analysis of Tablet (1:1 catalyst:binder)

After pressing the tablets, their strength was tested with a hardness tester (Company: Pharma Test; Type: PTB 311F). For this purpose, three tablets were tested at a production pressure of 2.5, 3.5 and 5 tons. The results are plotted in Figure 15. This figure shows that there is no significant increase of the strength of the tablets by increasing the pressure during the pressing. After several tablets, it turned out that the mixture of binder and catalyst wears off the die, which is why a new die with a diameter of 10 mm was used. Additionally, the composition of the catalyst and binder was changed to 2:1 for better reaction conditions. Therefore the pressure was raised to 8 tons to guarantee the same conditions of the 8 mm die. With the composition of 2:1 (catalyst:binder), the tablet stability is much higher than with the composition of 1:1, as seen in Figure 16.

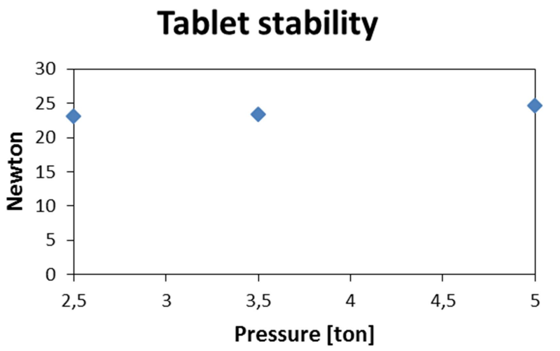

Figure 15: Tablet stability 1:1 (catalyst:binder), tested with hardness tester

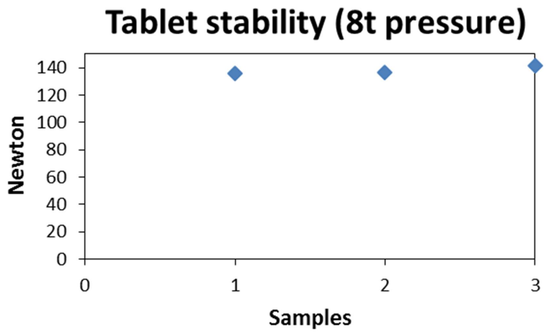

Figure 16: Tablet stability 2:1 (catalyst:binder), tested with hardness tester

Afterwards the pellets were crushed with different methods and different compositions to find a reproduceable way to achieve a particle size of about 1 mm. The first experiment was carried out with a tablet of pure catalyst and a pressure of 5 tons without a binder and pestled (see Figure 17). The tablet was very brittle and split irregularly. Then, a binder (calcium sulphate) was added and a composition of 1:1 (catalyst:binder) with a pressure of 5 tons were pestled (see Figure 18). The tablet did not split as irregularly, but with the pesteling, the size of the granulate was very inhomogeneous. Then, the amount of the catalyst in the tablet was increased to a ratio of 2:1 (catalyst:binder) to achieve a higher reactivity of the granulate by pressing with 5 tons. Next, the tablet was milled with a peppermill (see Figure 19) and sieved with a household strainer of a mesh of 0.7 mm to remove the fine fraction. This way, the granulate has a very good particle size distribution and is reproducible, but only a third of the mass of one tablet is left. This granulate is used for the Suzuki-Miyaura reactions.

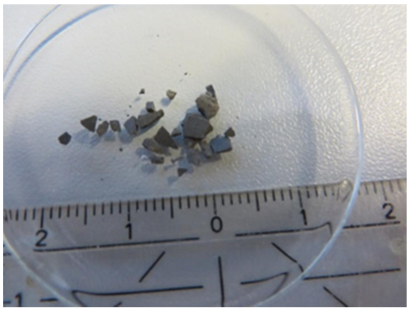

Figure 17: Tablet pure, pestled

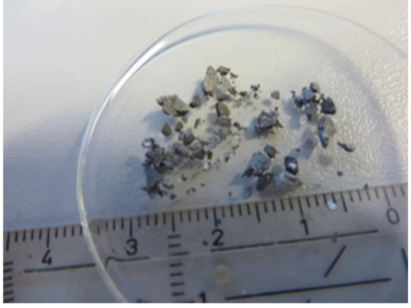

Figure 18: Tablet 1:1 (catalyst:binder), pestled

Figure 19: Tablet 2:1 (catalyst:binder), milled with peppermill

The granulate was investigated with QICPIC to get the particle size distribution (PSD) of the product (see Figure 20). The result showed that the distribution is closely around 1mm of the particle diameter.

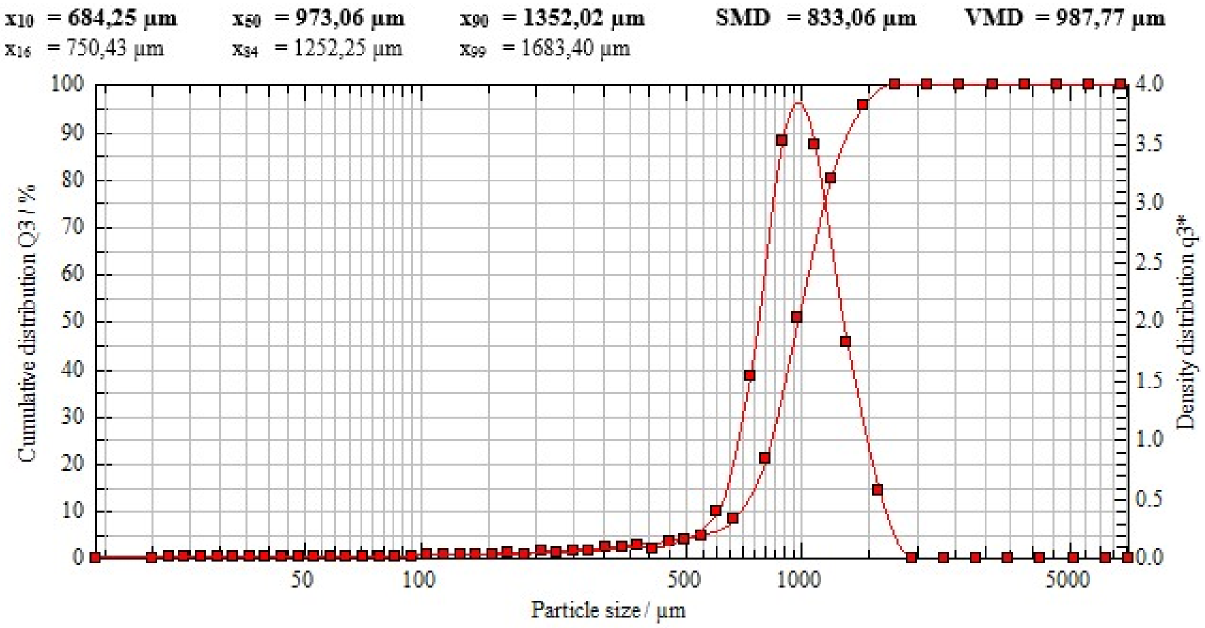

Figure 20: PSD of Tablet 2:1 (catalyst:binder), milled with peppermill

Specific surface area

The created granulate was investigated with a Tristar II 3020 (Micrometrics, Norcross, Georgia) to determine the specific surface area. This method works with nitrogen as analytical gas. At ambient temperature for 24 h the samples were degassed under vacuum. Over a relative pressure range between 0.01 and 0.99, the volume of nitrogen adsorption was recorded. According to the Brunauer-Emmet-Teller (BET) theory, 8 points in the relative pressure range of 0.05-0.2 were used for the calculation of the surface area. [5]

This led to a specific surface area of 26.2 m^2/g, which is a reduction of about the half compared to the pure catalyst of specific surface area of 54.8 m^2/g according to Georg Lichtenegger et al. [5]

3.2 Experimental details of the Suzuki-Miyaura batch reaction

During the batch-experiments, the chemical composition was the same but the amount and composition of the catalyst were different, which is why the behaviour of the granulate could be investigated (see Table 1). The Suzuki-Miyaura reaction was carried out using 4-bromotoluene and phenylboronic acid with the catalyst $Sn_{0.99}Pd_{0.01}O_{2-\delta}$, which leads to 4-methylbiphenyl. To compare the different catalysts, the turnover frequency (TOF) and number (TON) has been established. The big disadvantage of these numbers are that they varys with temperature, the concentration of substrate and other conditions [42]. The selectivity indicates the part of converted substrate compared to the generated product. The selectivity can only reach a maximum of 100%, but because of measuring inaccuracy it rises over 100%. Here, the selectivity is the quotient of yield, divided by conversion in percent.

Table 1: Summary of the results of the Suzuki-Miyaura batch experiments

Catalyst	amount Pd [µg]	preheating [°C]	t [h]	conv.[c] [%]	Yield [%]	Selectivity [%]	TON[a] [-]	TOF[b] [h^{-1}]
Powder*	0.0058	350	2	88.6	80.62	90.99	1854.60	927.30
Tablet pure**	0.1750	350	2	8.28	6.69	80.80	4.89	2.45
Tablet (1:1)***	0.0875	350	2	0.73	0.81	110.96	1.20	0.60
Gran. 150 mg	0.1167	350	2	91.01	94.9	104.27	111.21	55.61
Gran. 75 mg	0.0583	350	2	70.13	79.6	113.50	186.08	93.04
Gran. 37.5 mg	0.0292	350	2	77.02	79.3	102.96	352.15	176.07
Gran. 150 mg	0.1167	550	2	75.84	76.56	100.95	77.27	38.64
Gran. 150 mg	0.1167	650	2	89.6	91.47	102.09	106.71	53.36

[*] Powder: amount of 5mg catalyst; [**] Tablet: amount of 150 mg catalyst; [***] Tablet(1:1) amount of 75 mg catalyst

[a] Moles of 4-methylbiphenyl produced per mole of catalyst [34]
[b] Moles of 4-methylbiphenyl produced per mole of catalyst per hour[34]
[c] Conversion of 4-bromotoluene

Evaluation of the batch- results:

As starting conditions for evaluating the granulate, 5 mg of pure catalyst powder was used (see Figure 21). To reach the same conversion, an amount of about 150 mg granulated catalyst (about 0.117 mg Pd) is necessary (see Figure 22). To obtain the same results with the granulate, the amount of palladium was about 20 times higher than that of pure catalyst-powder.

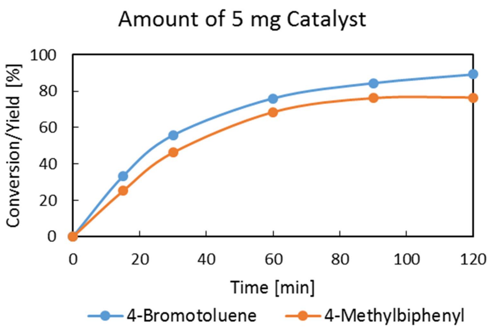

Figure 21: Suzuki: Conversion with an amount of 5mg Catalyst at a temperature of 75°C

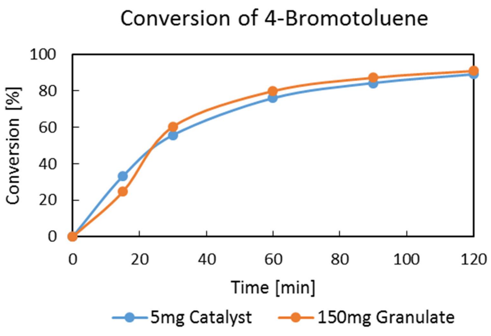

Figure 22: Suzuki: Conversion with different amount of catalyst at a temperature of 75°C

Next, different amounts of granulate were tested to discover the influence of the conversion. As can be seen in Figure 23, the conversion at the end is rather similar, especially between 75 mg and 37.5 mg. A considerable difference can be noted during the first hour of the experiment.

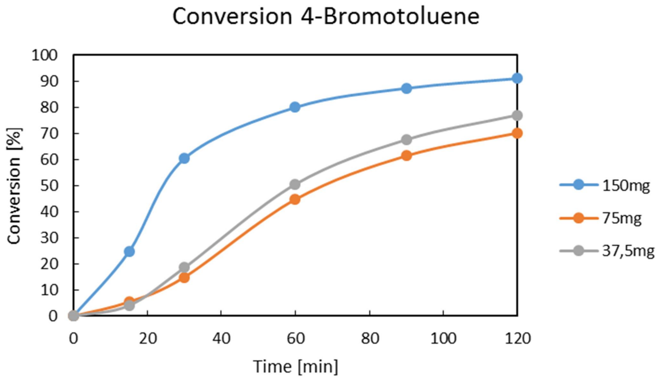

Figure 23: Suzuki: Conversion of 4-bromotoluene with different amounts of granulate

The influence of the temperature dependency of the catalyst activity as a result of preheating is shown in Figure 24. In general, the catalyst, which was preheated at 650°C was better than the catalyst at standard conditions (350°C). Only the catalyst preheated at 550°C does not work as well as the standard and the preheated 650°C catalyst.

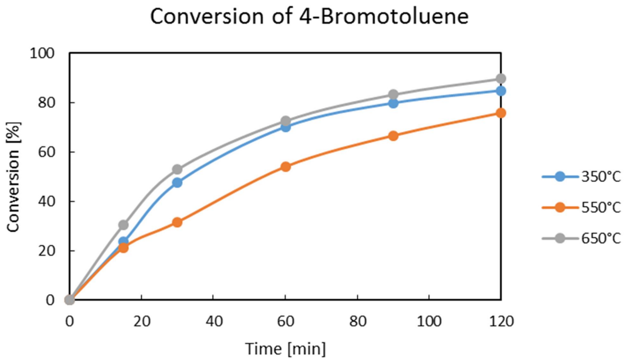

Figure 24: Suzuki: Conversion of 4-bromotoluene with different granulated catalyst that were preheated of different temperatures.

3.3 Heck reactions in batch

During the batch-experiments, the chemical composition was the same but the amount and composition of the catalyst were different. In order to study the behaviour of the granulate (see Table 3).

Table 2: Summary of the results oft he Heck batch experiments

Catalyst	amount Pd [µg]	preheating [°C]	t [min]	conv.[c] [%]	Yield [%]	Selectivity [%]	TON[a] [-]	TOF[b] [h^{-1}]
Gran. 150 mg	0.1167	350	2	83.41	42.35	50.77	48.01	24.01
Gran. 300 mg	0.2333	350	2	74.3	44.32	59.65	18.05	9.03
Gran. 150 mg	0.1167	550	2	83.2	43.64	52.45	46.06	23.03
Gran. 150 mg	0.1167	650	2	88.79	65.29	73.53	60.36	30.18
Powder 5 mg	0.0058	650	2	75.55	44.44	58.82	1067.71	533.85
Gran. 150 mg*	0.1167	550	2	83.41	39.65	47.54	44.99	22.49
Gran. 150 mg	0.1167	350	24	96.53	42.21	43.73	52.22	2.18

*standard stock solution with different base: Cs_2CO_3

[a] Moles of 4-Phenyl-but-3en-2-ol product per mole of catalyst [34]
[b] Moles of 4-Phenyl-but-3en-2-ol product per mole of catalyst per hour [34]
[c] Conversion of Iodobenzene

In the first experiment, an amount of 150 mg of granulated catalyst (0.117 mg Pd) preheated at 350°C was chosen (similar to Suzuki-batch experiment). In spite of the good conversion, the yield was only half of the converted iodobenzene, as can be seen in Figure 25. By using GC for analysis, it turned out that a ketone (4-Phenyl-but-3-en-2-on) was formed as a side product.

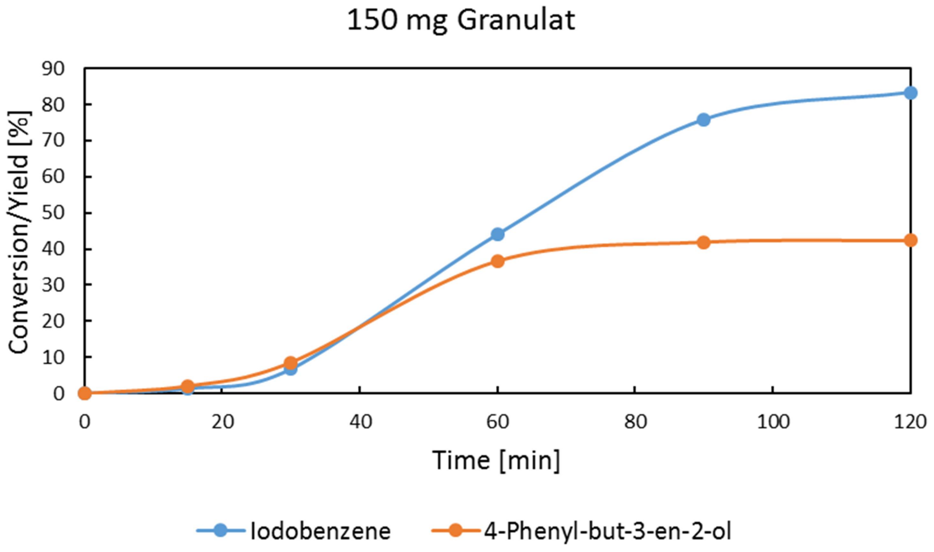

Figure 25: Heck: Conversion/Yield at 150mg granulate

By using the double amount of granulate, the conversion increases, but the selectivity remains about 50 %. The experiment was carried out with a pure catalyst and the result was the same, which means that the binder has no influence on producing a side product. In addition, preheating the catalyst at 550°C and 650°C does not mean better selectivity, but a slight increase in the performance of the catalyst. In the next step, the base was changed from potassium carbonate to cesium carbonate, so the result shows that the base also does not influence the side product. The long-time experiment (24 h) led to the result that the conversion and yield of this reaction does not increase anymore after 2 hours.

3.4 Continuous Suzuki reaction

Before the continuous Suzuki reactions were carried out, the behaviour of the Plug & Play reactor was analysed.

Residence time distribution:

The step function was chosen to measure residence time. Hence, two stock solutions with a composition of Ethanol:H_2O 7:3 as used in the experiments were prepared. One of the two solutions was prepared with anisole to measure the concentration over time and to guarantee a fast switch to the tracer. For a good resolution, samples were taken every two minutes. The residence time was measured for two columns filled with granulate and flow rates of 0.45 ml/min and 0.5 ml/min.

The evaluation of the residence time was carried out with HPLC. Every experiment was conducted for 30 minutes. Based on the measured data, the mean residence time (tm) (Eq. 3), the variance (σ^2) (Eq. 5), and the Bodenstein number (Bo) (Eq. 6) were calculated, as listed in Table 3.

Table 3: Residence time distribution, experimental details and results

vol. flow [ml/min]	columns [-]	granulate [g]	tm [min]	$\sigma(t)^2$ [s^2]	$\sigma(\Theta)^2$ [-]	Bo [-]
0.5	2	6.0247	7.962	4.728	0.0746	30.353
0.45	2	6.0247	8.461	7.721	0.1078	21.927
0.45	3	7.8858	11.322	4.823	0.038	56.887
0.45	1	2.5647	7.278	8.167	0.154	16.177

The residence time distribution (E-function) (see Figure 26) and the calculated F-function (see Figure 27) for the two flow rates of the two columns with the same amount of granulate are pictured below. These results were shown in an overlay layer to demonstrate the dependence of the volumetric flow on the residence time. In addition, it can be seen in Table 3 that the mean residence time increases by lowering the flow rate and that residence time (tm) is about 8 min for 2 columns filled with granulate, which is similar to the findings reported by Lichtenegger et al. [2].

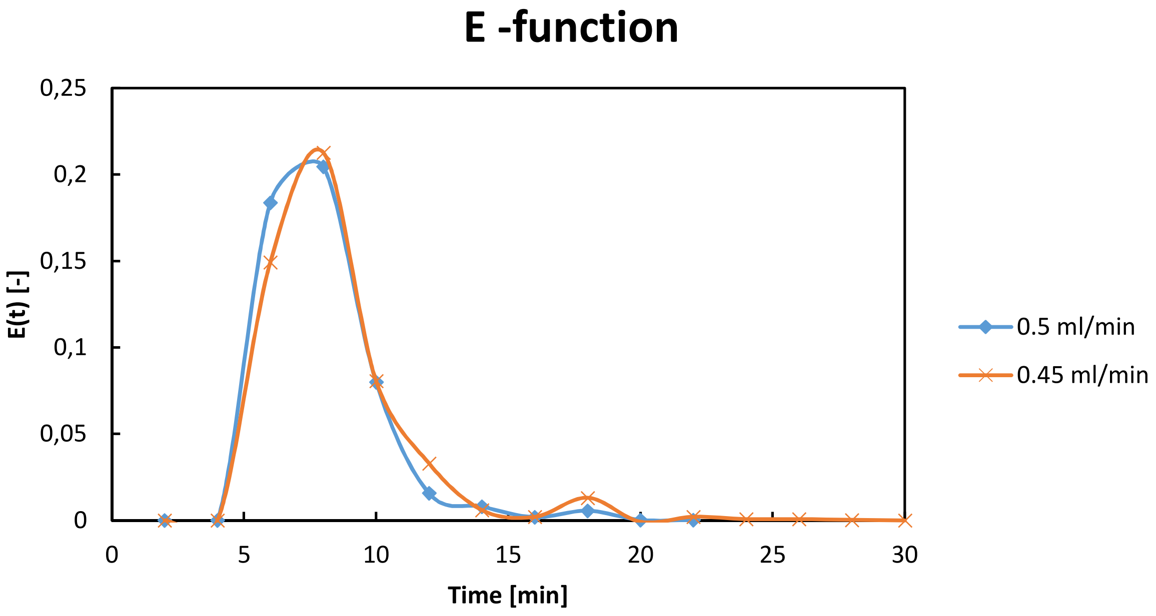

Figure 26: E-function at different flow rates

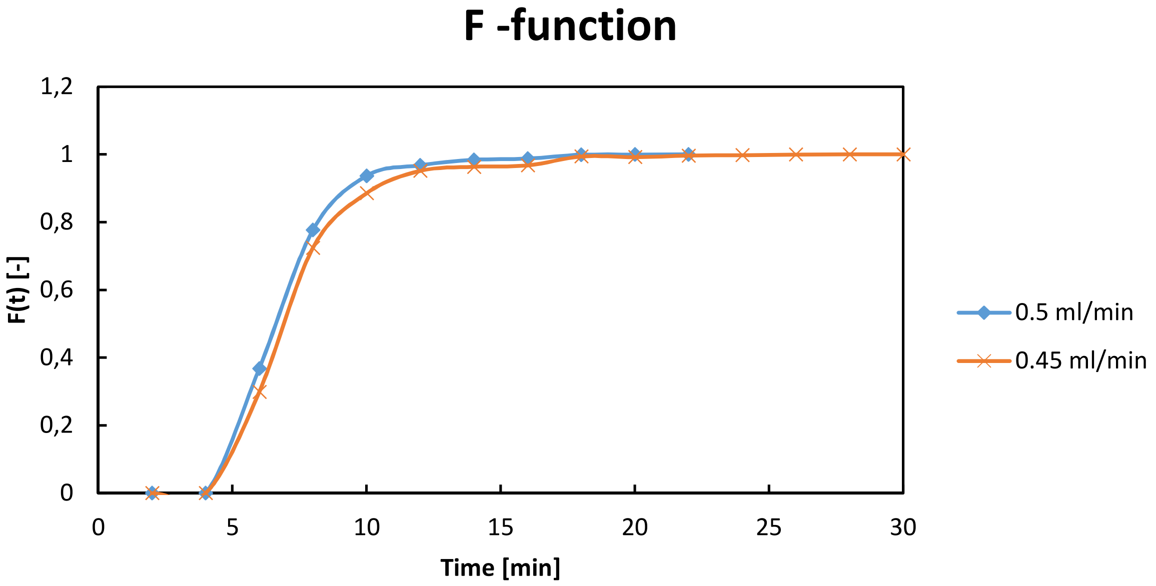

Figure 27: F-function at different flow rates

Next, the residence time distribution (E-function) (see Figure 28) and the calculated F-function (see Figure 29) for the same flow rate, but with different numbers of columns, were compared.

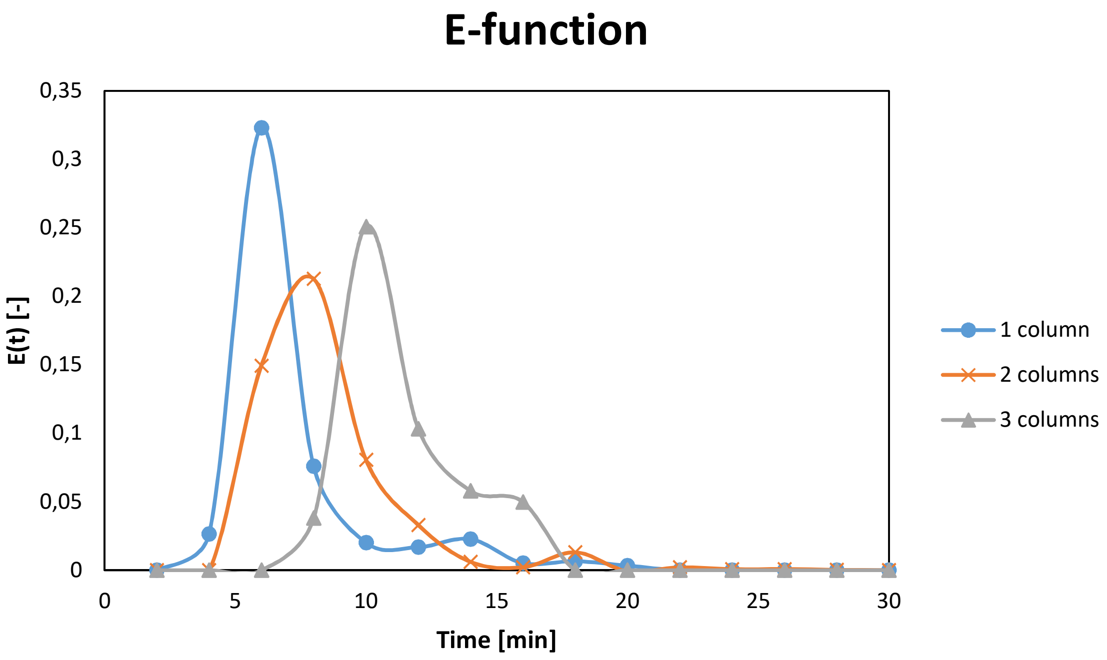

Figure 28: E-function with different amounts of columns

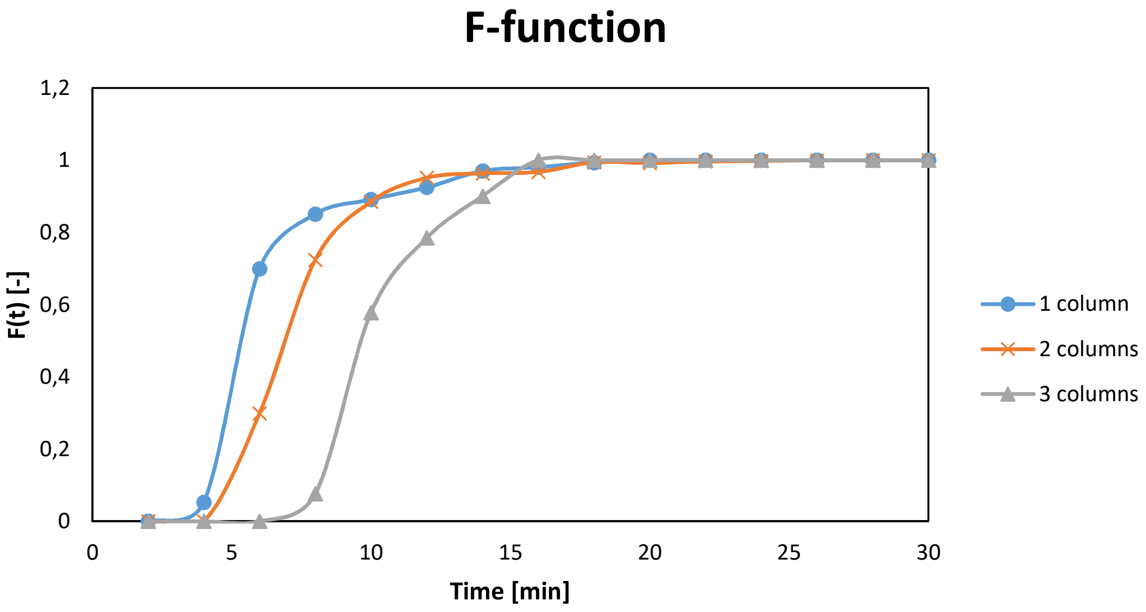

Figure 29: F-function with different amounts of columns

The mean residence time and the variance are summarized and plotted in Figure 30. Here, the mean residence time increased with the number of columns but not linearly at the same flow rate, while the variance decreased. This means that the spread of the distribution and therefore the dispersion decreases with the number of columns. This effect can also be seen at the Bodenstein number, which increases with the number of columns, indicating that the back mixing decreases.

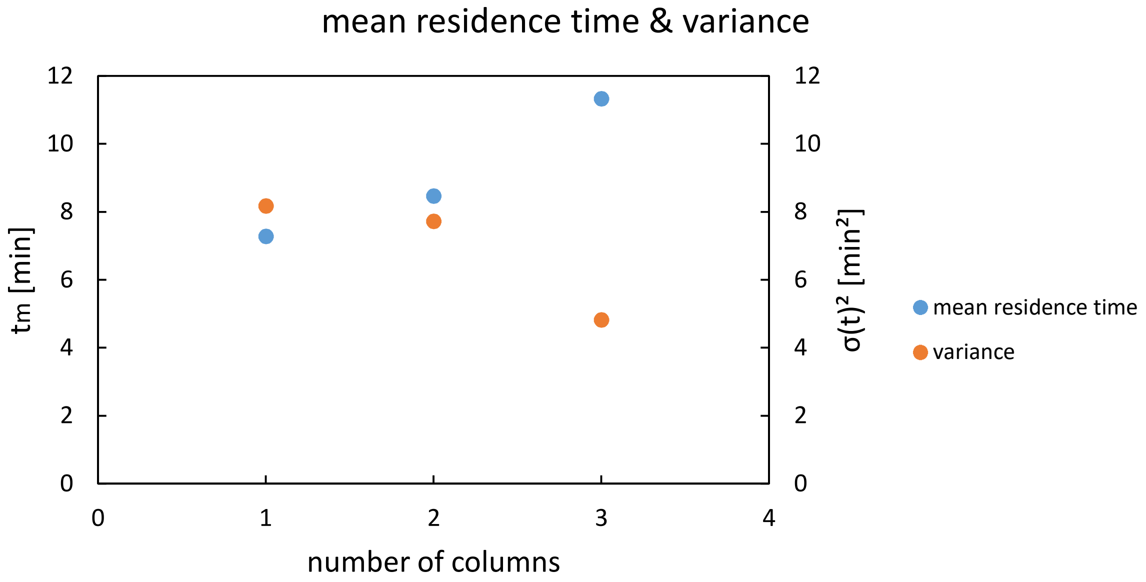

Figure 30: Mean residence time and variance with different columns

Key parameters for packed bed reactors:

In order to calculate the bed porosity (Eq. 10), the particle volume fraction (Eq. 9) and the relative catalyst volume (Eq. 11), the mass of granulate in the column, and the repressed mass of water in the column from the catalyst were measured. The measured data and calculated parameters are represented in Table 4.

Table 4: Key parameters for packed bed reactors

	vol. column	mass granulat	mass water	vol. water [V_l]	vol. granulat [V_p]	bed porosity [ε]	particle volume fraction [φ_p]	relative catalyst volume [Y_p]
#	[mm³]	[g]	[g]	[mm³]	[mm³]	[-]	[-]	[-]
1	1774	2.5647	1.136	1136	638.37	0.640	0.360	0.562
2	1774	2.6985	1.068	1068.7	705.67	0.602	0.398	0.660
3	1774	2.6626	1.011	1010.8	763.57	0.570	0.430	0.755
4	1774	2.5009	1.209	1209.1	522.84	0.698	0.302	0.432
					Average:	0.628	0.372	0.602

Continuous flow experiments:

During the continuous experiments, the composition of the starting stock solution was the same as in the batch experiments and the temperature was kept at 75°C. A different amount of columns and masses of catalyst over different flow rates were used to determine the behaviour of granulate during continuous process conditions. Table 5 provides an overview of the different experiments that were carried out.

Table 5: Continuous flow experiments, experimental details

#	columns [-]	amount granulate [g]	amount Pd [mg]	vol. flow [ml/min]	Time [min]	Conversion [%]	Yield [%]
1	1	3.0837	0.0024	0.5	75	20	18
2	2	5.0907	0.0040	0.2/0.1	75/75	15/25	15/23
3	2	6.1127	0.0048	0.5/0.2	180/120	32/40	31/35
4	3	9.0779	0.0071	0.45	300	20	18

The first experiment was carried out to discover the reachable conversion and yield with one column and a flow rate of 0.5 ml/min. The results are displayed in Figure 31.

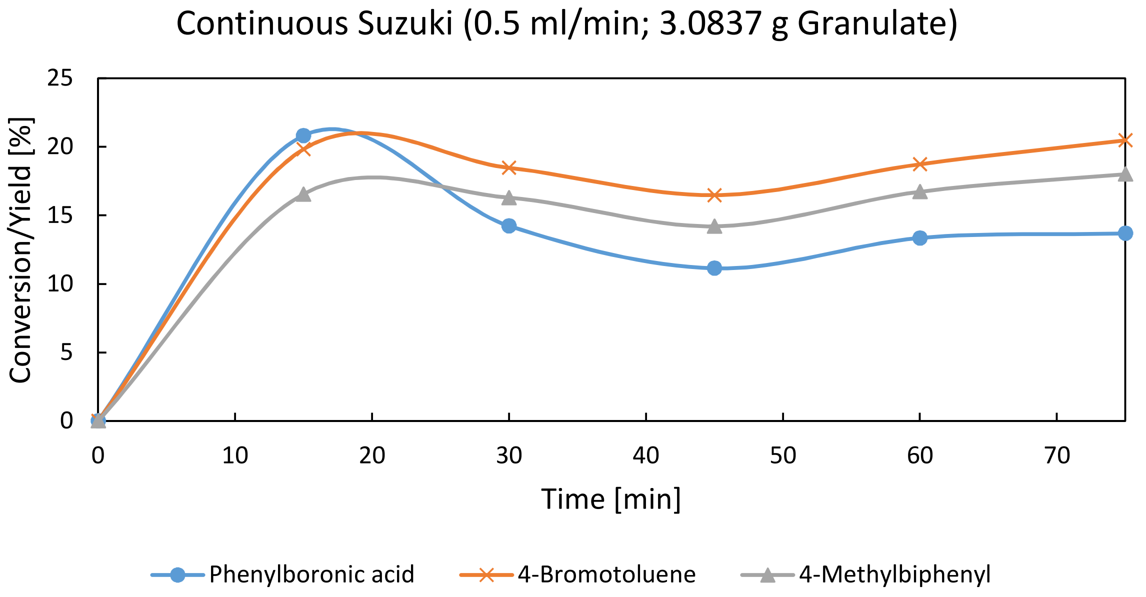

Figure 31: Conversion/Yield at a flow rate of 0.5ml/min with one column and at a temperature of 75°C

During the second experiment, the flow rate was changed from 0.2 ml/min to 0.1 ml/min after 75 minutes. In addition, a second column was installed to expand the residence time and to achieve a better conversion, as shown in Figure 32. On the left side of the grey bar, the flow rate of 0.2 ml/min is illustrated, while the right side shows the flow rate of 0.1 ml/min.

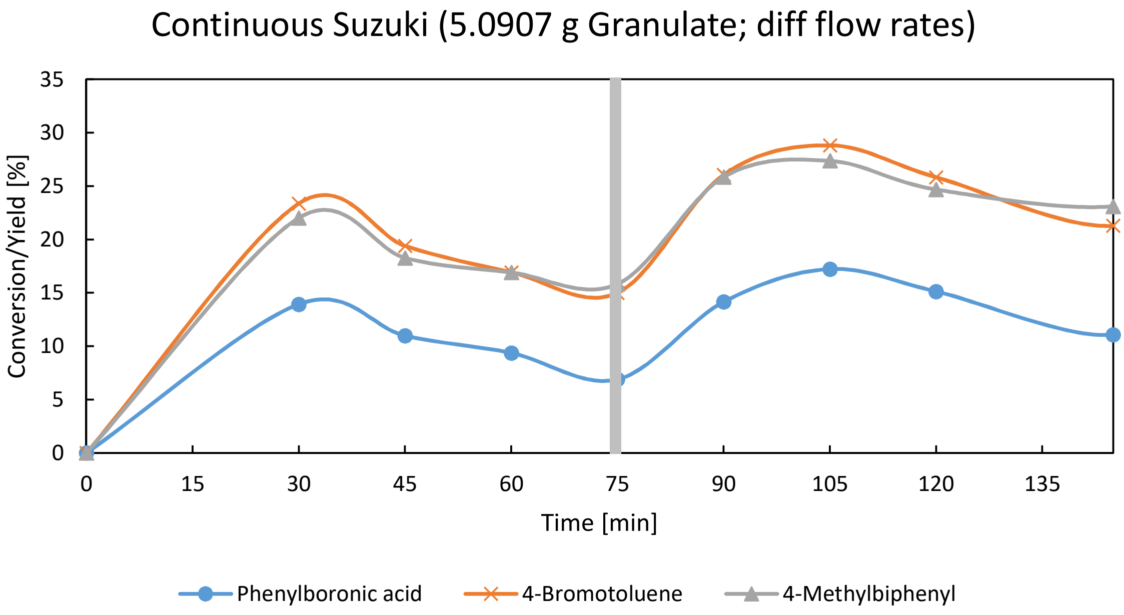

Figure 32: Conversion/Yield with two columns at flow rates of 0.1 ml/min and 0.2 ml/min

For the third experiment, two columns were used as well, but the flow rate was set at a higher level. During the first 180 minutes, a flow rate of 0.5 ml/min was chosen, which was lowered to 0.2 ml/min afterwards because the equilibration was not reached after 180 minutes. Additionally, the pressure was measured during the experiment. As can be seen in Figure 33, the pressure dropped when the flow rate was set at a lower level, but even after 180 minutes, a constant conversion could not be achieved.

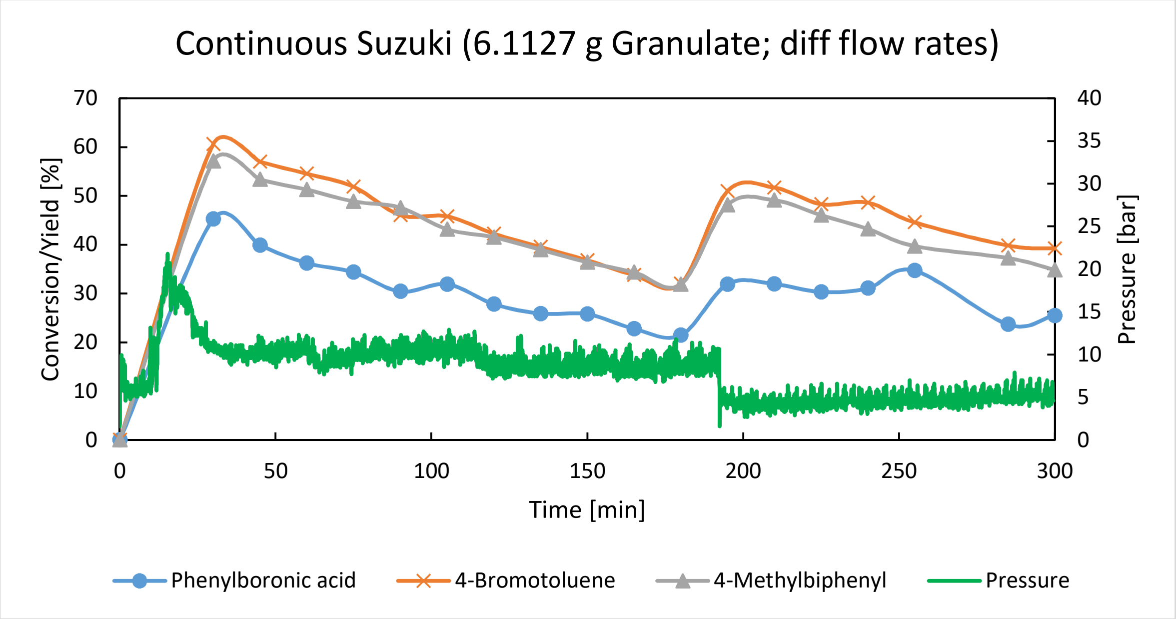

Figure 33: Conversion/Yield with two columns at different flow rates and pressure

The last experiment was carried out over a period of 300 minutes at a constant flow rate of 0.45 ml/min and with three columns. It takes at least about 260 minutes for a constant conversion to adjust itself, as Figure 34 shows.

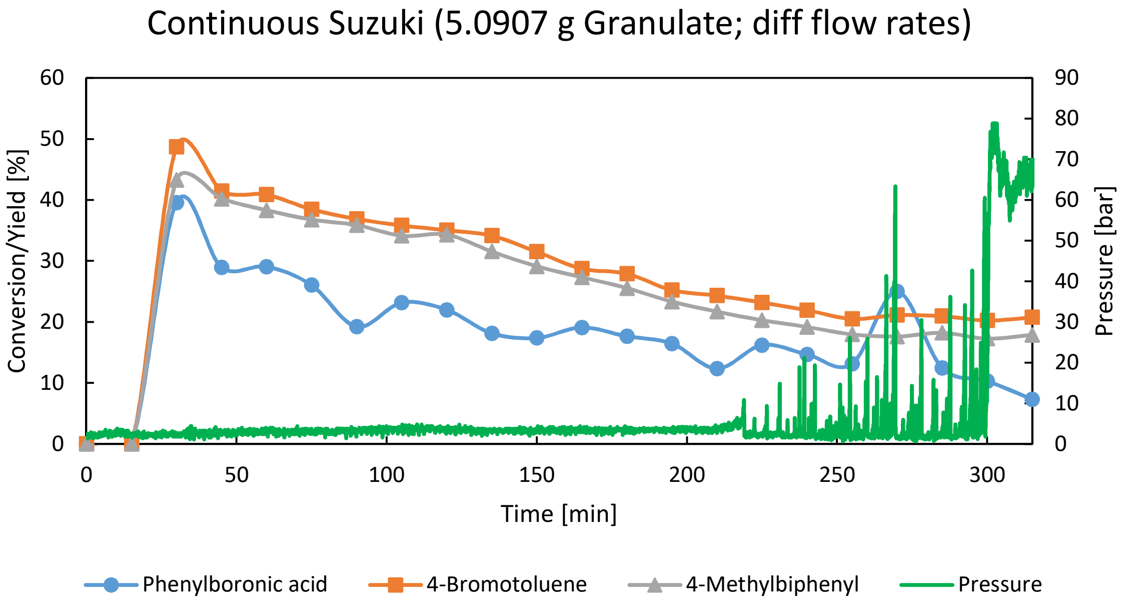

Figure 34: Conversion/Yield with three columns at a constant flow rate

During the continuous experiments, the conversion and yield was about 20%. As a consequence, this catalyst ($Sn_{0.99}Pd_{0.01}O_{2-\delta}$) works very well in batch experiments, but the performance in the continuous experiments was not so good. According to Georg Lichtenegger et al. [5], the catalyst $Sn_{0.99}Pd_{0.01}O_{2-\delta}$ works best in batch reactions, but for continuous experiments the catalyst was changed to $Ce_{0.495}Sn_{0.495}Pd_{0.01}O_{2-\delta}$ to get a better performance. Nevertheless the granulate seems to be applicable also in continuous processes.

4 Experiments

4.1 Catalyst Synthesis

To synthesize 3 g of catalyst ($Sn_{0.99}Pd_{0.01}O_{2-\delta}$), 4.077 g SnC_2O_4, 0.035 g $PdCl_2$ and 3.307 g Glycine were used. For this purpose, the ingredients were scaled and pesteled. Afterwards, the mixed chemicals were filled in a 600 ml beaker and put in an ultrasonic bath for 30 minutes. Then, the beaker was put in a furnace at 350°C for one hour. The catalyst was then pesteled again and put back into the oven at the same temperature for 24 hours.

4.2 Granulation

For the granulation, four different methods were carried out. In the first method, the catalyst is agglomerated with different binders, the second method is coating some pellets with the catalyst combined with a binder. The third method is to press the catalyst combined with a binder to tablets and grind them to the required particle size. Finally, sintering is carried out to fix the catalyst to the carrier with a thermal treatment. 7

4.2.1 Agglomeration

For agglomeration, three different binders, potassium carbonate, dextrin and alginic acid sodium salt were investigated. To agglomerate the catalyst with the binder, high-shear agglomeration was carried out. The catalyst is merged in dry form with the binder and under mixing, the compound is sprinkled with water for agglomeration. Every experiment was prepared separately with the same composition (catalyst:binder 2:1). 0.9 g Catalyst (Kat2, 6.11.2015 (Ofenboden)) were mixed with 1.8 g binder.

Experimental setup

For mixing the merged dry compounds were filled into a snap cover glass, which was fixed to a heating plate (Type IKA C-MAG HS7 digital). Then an agitator (Type CAT r50) was mounted for high-shear mixing, as can be seen in Figure 35. After starting the agitator, water was added drop by drop. At the same time, the magnetic stirrer was heated up to 140°C to guarantee smooth drying during agglomeration. These experiments were carried out with two different types of stirrers, an axial and a radial stirrer as shown in Figure 36.

Figure 35: Experimental setup agglomeration

Figure 36: Used stirrer for agglomeration, left: axial stirrer, right: radial stirrer

4.2.2 Coating

For coating, the pellets were rolled in a slurry of catalyst and binder. Potassium carbonate, dextrin and alginic acid sodium salt were used as a binder. Furthermore, gravel pellets, glass pellets and alumina oxide pellets were used. Afterwards, the coated pellets were dried in a furnace to create a solid coating. Another method is to moisture the pellets with the binder and roll them in dry catalyst. The glass pellets had a diameter of 1.5 to 1.85 mm, the gravel was ranged between one to two millimetres, and the alumina oxide pellets had an average diameter of three millimetres and a length of four millimetres. The blend of catalyst and binder for the slurry was 1:1 (0.7 g catalyst: 0.7 g binder). For moistening the pellets, a saturated solution with water and binder was prepared.

Experimental setup

For drum granulating (see Figure 37), a can was mounted on an agitator to create a drum granulator. This way, the pellets can roll over the moisture of the catalyst and binder to coat them homogeneously. However, it is also possible to spray the moisture on the rolling pellets for coating. Afterwards the coated pellets were dried in a compartment dryer (Type Memmert).

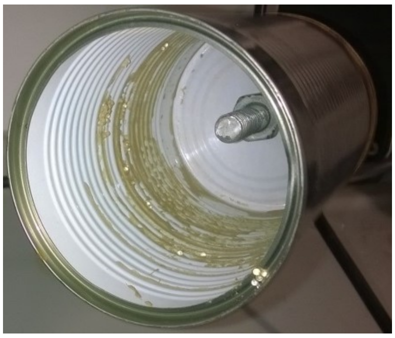

Figure 37: Drum granulator

4.2.3 Sintering

This method aimed to sinter the catalyst directly on the pellets during production. This way, the slurry of raw catalyst diffuses into the pores and stacks there while it is heated in the oven up to 350°C to get fixed.

4.2.4 Pressing and Milling

To accomplish this, a tablet press (Company: Maassen GmbH, Type 25T hydraulic) was used with a die of 8 mm diameter and 10 mm diameter. For pressing, the catalysts were mixed with a binder (Calcium sulphate) and about 150 mg of different mixtures were filled into the die. Next, it was pressed with different amounts of pressures to characterize the tablet strength. During pressing, the pressure was held for about one minute during the compaction stage. Afterwards, the tablets were milled (Peppermill CLASSIC I) to the demanded particle size.

4.3 Suzuki-Miyaura and Heck reaction

4.3.1 Experimental setup batch reaction for Suzuki

All experiments followed the same procedure and every batch was prepared separately. Substrate 1 (4-Bromotoluene) (0.7 mmol) was dissolved in the reaction solvent (20 ml ethanol:H_2O 7:3) to achieve a starting concentration of 35 mmol/L. The second substrate (phenylboronic acid) and the base (potassium carbonate) were added with 1.5 mol equivalents (1.05 mmol) and also 100 µL Anisole (internal standard). A 50ml round bottom flask with two entrances was used to add the reactants and the internal standard into without catalyst. The flask was fixed in an oil bath with a magnetic stirrer. For mixing the solution, an agitator was mounted above, stirring it from the top. To control the temperature and to keep it at 75°C, a thermostat was dipped into the oil bath. Before adding the catalyst and after reaching the reaction temperature, a blank sample was taken. The stirrer speed was adjusted so that the catalyst and the solvent could be mixed very well. To monitor the reaction progress, samples from the reaction solution (100 µl) were taken after 15, 30, 60, 90, and 120 minutes and analysed with a HPLC. For preparing the samples, the reaction solution (100 µl) was diluted in 1 ml of the eluent in accordance with the chosen HPLC-method.

4.3.2 Experimental setup batch reaction for Heck

For the Heck-reaction, the same assumption for the stock solution was taken as for the Suzuki-Miyaura-reaction. Substrate 1 (iodobenzene) (0.7 mmol) was dissolved in the reaction solvent (20 ml ethanol:H_2O 7:3) to achieve a starting concentration of 35 mmol/L. The second substrate (3-butene-2-ol) and the base (potassium carbonate) were added 1.5 mol equivalent (1.05 mmol) and also 100 µL anisole (internal standard). A 50 ml round bottom flask with two entrances was used to weigh the reactants and the internal standard into without catalyst. The flask was fixed in an oil bath. For mixing the solution, an agitator was mounted above, stirring it from the top. To control the temperature and to keep it at 80°C, a thermostat was dipped into the oil bath. Before adding the catalyst and after reaching the temperature, a blank sample was taken. The stirrer speed was set so that the catalyst and the solvent were mixed very well. To monitor the reaction progress, samples from the reaction solution (100 µl) were taken after 15, 30, 60, 90, and 120 minutes and analysed with a HPLC. For preparing the samples, the reaction solution (100 µl) was diluted with 1ml of the flow control agent in accordance with the chosen HPLC-method.

4.3.3 Experimental procedure for continuous Suzuki reaction

The continuous processes for the Suzuki-Miyaura reaction had the same composition of the stock solution as the batch experiments, only the volume of the solution changed, depending on the flow rate and experimental duration. During the continuous process, samples were taken every 15 minutes and prepared for HPLC analysis, as described in the batch experiments. The amount of catalyst depends on the number of columns which were used in the reactor. In the reactor, a maximum number of three columns could be mounted, each of them with an inner diameter of 8 mm and a length of 40 mm. The used backpressure regulator was set to 75 psi, which is equivalent to about 5 bar.

The first continuous experiment was carried out with one column over a period of 75 minutes and a flow rate of 0.5 ml/min. The backpressure regulator was mounted to reach a constant flow during the experiment. A stock solution of 100 ml was prepared and the column was filled with 3.083 g granulated catalyst (0.00239 mg Pd).

The second experiment was carried out with two columns and different flow rates. The first flow rate was chosen with 0.2 ml/min without a backpressure regulator at the end over a period of 75 minutes. The second flow rate was set to 0.1 ml/min without a backpressure regulator at the end over a period of 75 minutes. At the end, the flow rate was set at 0.2 ml/min once again for 30 minutes and the backpressure regulator was mounted. During these experiments, the amount of granulated catalyst was 5.09 g (0.00396 mg Pd).

Then, a continuous experiment with two columns and a backpressure regulator downstream was carried out. The first part had a flow rate of 0.5 ml/min over a period of three hours. In the second part, the flow rate was lowered to 0.2 ml/min for two hours. The total amount of granulated catalyst during the experiment was 6.112 g (0.00475 mg Pd).

The long-term experiment had an experimental time of five hours with three columns and a backpressure regulator. During this time, the mass flow was constant at 0.45 ml/min with a load of 9.078 g of granulated catalyst (0.0071 mg Pd).

Residence time distribution measurements:

The step function was chosen to measure residence time. Hence, two stock solutions with a composition of Ethanol:H_2O 7:3 as used in the experiments were used. One of the solutions was prepared with anisole to measure the concentration over time, the other solution without anisole was the reference solution. For a good resolution, samples were taken every two minutes. The residence time was measured for two columns and flow rates of 0.45 ml/min and 0.5 ml/min.

Measurements to calculate key parameters for packed bed:

One column was used to repeat the measurement several times. The mass of granulate filled in the column and the amount of water in the column with catalyst were measured. These measurements were carried out four times to obtain average values to calculate the key parameters.

4.4 Plug &Play reactor

The Plug&Play reactor [32], in which the continuous Suzuki reaction was carried out, consists of an integrated reactor heating to enable a constant reacting temperature. Drillings in the alumina block ensure the heating of the column. The educts were preheated in meandering formed tubes through the block before they got into the columns with the catalyst. The following figure illustrates the Plug&Play reactor (Figure 38).

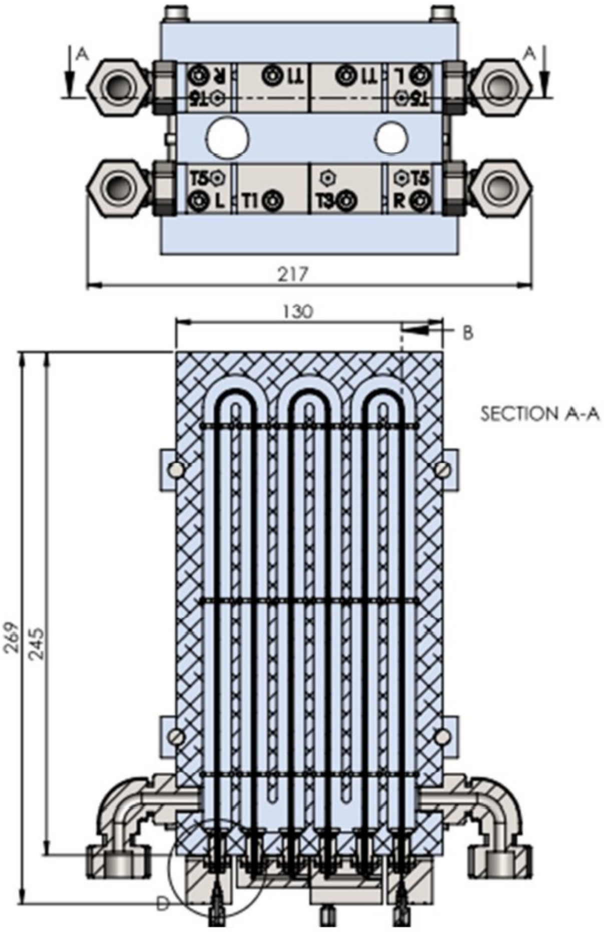

Figure 38: Sketch of Plug&Play reactor [32]

The column of the reactor with an inner diameter of 8 mm and a length of 40 mm is a HPLC-column and consists of a tube with detachable lids at the ends. In the middle, there is a sieve and a sealing. The column can be removed very easily from the reactor because it had to be refilled with catalyst several times. [32]

4.5 Analysis

4.5.1 Method for Suzuki-Miyaura reactions

The evaluation of the results was carried out by high performance liquid chromatography (HPLC). According to the used method and solvent, a calibration for all occurring substances had to be carried out, as seen in the appendix. Afterwards the method for HPLC is explained.

HPLC-Method:

The HPLC analysis was carried out with an Agilent 1100 series HPLC system (Agilent, Waldbronn, Germany) equipped with an online degasser, quaternary pump, autosampler, thermostatted column compartment, and a UV-visible diode array detector. An Agilent Poroshell 120 EC-C18 reversed phase column (50x4.6 mm; 2.7 µm) was used as a stationary phase. The analysis was carried out under gradient elution conditions using a mobile phase consisting of methanol and aqueous phosphoric acid (water:phosphoric acid = 300:1 v/v). The corresponding elution program is given in Table 6.

Table 6: Used method for HPLC to analyze Suzuki and Heck reactions

Time [min]	%A (v/v)	%B (v/v)	Flow [ml/min]
0	40	60	1
3	40	60	1
9	80	20	1
11	80	20	1
13	40	60	1

Used HPLC method applying solvents A (methanol) and B (water:phosphoric acid = 300:1 v/v)

The column temperature was set at 25°C. An aliquot of 2 µL of the sample solution was injected into the HPLC system. UV-detection was performed at 237 nm over a run time of 16 minutes. [5]

4.5.2 Method for Heck reaction

The evaluation was carried out with HPLC analyses, as described in the HPLC-Method. In addition to HPLC, gas chromatography (GC) was performed, because 3-butene-2-ol is not visible in the HPLC. For this purpose, the GC-method as described below was used.

GC-Method:

The GC analysis was done by using a Perkin Elmer Clarus 500 equipped with an Optima HP 5-MS 0.25 µm column (30m x 0.32 mm ID capillary column), an autosampler, and a flame ionization detector. The detector needs H_2 (45ml/min) and synthetic air (450ml/min) in order to work. The analysis was carried out under linear elution conditions, using nitrogen as mobile phase. The corresponding elution program started at a temperature of 50°C, held it for 5 minutes and then started to heat up to 200°C with a rate of 10°C/min. At the end, the temperature of 200°C was held for 2 minutes, the whole method took 22 minutes. The injection volume was 1 µl at an injector temperature of 250°C. N_2 was used as a carrier gas at a flow rate of 2ml/min.

5. Conclusion and outlook

In this work, the heterogeneous catalyst $Sn_{0.99}Pd_{0,01}O_{2-\delta}$, developed by Georg Lichtenegger et al.[5] had to be granulated to an average particle size of 1 mm. This is necessary at continuous processes to simplify the downstream process. Therefore, a screening of different granulating technologies and types of binders was done. In the end, the decision was made for pressing and milling, because it led to the best results under the given conditions, respectively to PSD and high mechanical strength of the granulate. A narrow PSD is necessary for continuous processes when granulate is used in a packed bed reactor to reach homogeneous process conditions. The mechanical strength of granulate is needed to keep the form of granulate during the operation and to avoid catalyst leaching.

The granulated catalyst was evaluated in several batch experiments, using Suzuki-Miyaura and Heck reactions. For this purpose, the stock solution of the particular reaction was kept constant and the amount of catalyst was changed.

Then, the granulates were tested in a continuous process by using the Suzuki-Miyaura reaction. This happened in the so called Plug&Play reactor. The advantages of this type of reactor are that the temperature for the reaction could be kept at a constant level and that, by installing up to three columns, the amount of catalyst could be easily changed.

The results of the continuous flow experiments show that it takes a very long time (at least about four hours) to reach steady state conditions. Unfortunately, the conversion only reaches a level of 20 percent, even when all three columns filled with granulate are in use.

For further work in this area, it is recommended that the granulating process is changed and to use coating instead of pressing and milling. This would lead to a reduction of the used catalyst, depending on the thickness of the washcoat. Also, an increase in the residence time in the reactor will help to generate more yield. This can be done by reducing the volumetric flow or increasing the active length of the packed bed reactor.

Bibliography

[1] Maksym O. *Heterogeneous Pd catalyst supported on silica matrices*., Royal Society of Chemistry, 2014

[2] Georg J. Lichtenegger *Continuous Suzuki–Miyaura Reactions with Novel Ce–Sn–Pd Oxides and Integrated Crystallization as Continuous Downstream Protocol*., J Flow Chem., 2016

[3] Sun Qi *Porous polymer supported palladium catalyst for cross coupling reactions with high activity and recyclability.,* Science China Chemistry 55, 2095 , 2012

[4] David Cantillo, C. Oliver Kappe *Immobilized Transition Metals as Catalysts for Cross-Couplings in Continuous Flow—A Critical Assessment ofvthe Reaction Mechanism and Metal Leaching.,* ChemCatChem, 6, 3286-3305, 2014

[5] G. J. Lichtenegger *Suzuki-Miyaura coupling reactions using novel metal oxide supported ionic palladium catalysts*., Journal of Molecular Catalysis A: Chemical 426, 39-51 , 2017

[6] Henk G. *Production, Handling and Characterization of Particulate Materials*, Volume 25, Paricle Technology Series, Springer, 2016

[7] Litster J. *The Science and Engineering of Granulation Processes*., Particle Technology Series, Springer, 2004

[8] Nick Jones *Sensitives in Wet Granulation Processes*., CET IIB Research Project, University of Cambridge

[9] Kapur, P.C. *Balling and granulation* , Adv. Chem. Eng. 10, 55–123, 1978

[10] Newitt D.M. *A contribution to the theory and practice of granulation*, Trans. Inst. Chem. Eng. 36, 422–442, 1958

[11] Michaels J.N., et al. *Steady states in granulation of pharmaceutical powders with application to scale-up*, Powder Technol. 189(2), 295–303, 2009

[12] C. Elik M. *Pharmaceutical Powder Compaction Technology*, 2nd edn, CRC Press, Boca Raton (2011)

[13] Duberg M. *Studies on direct compression tablets XII. The consolidation and bonding properties of some pharmaceuticals compounds and their mixtures with Avicel 105* , Int. J. Pharm. Technol. Prod. Manuf., 6:17, 1985

[14] El Grindy NA *Tensile strength of some pharmaceutical components and their relation to surface free energy* , Int. J. Pharm. , 13:35-46, 1983

[15] Rumpf H. *Basic principles and methods of granulation*, I. II. , Chem. Eng. Tech. 30:144, 1958

[16] Führer C. *Substrate behaviour in direct compression*, Lab. Pharma Probl. Technol. 269:759, 1977

[17] Kurt A. Rosentrater "*Kent's Technology of Cereals, An Introduction for Students of Food Science and Agriculture*", Fifth Edition, Publishing Series in Food Science, Technology and Nutrition, Woodhead Publishing, 2018

[18] Sunil S. Joshi *Industrial Catalytic Processes for Fine and Specialty Chemicals*, Elsevier, 2015

[19] C. Torborga *Recent applications of palladium-catalyzed coupling reactions*, Adv. Synth. Catal. , 351, 3027–3043, 2009

[20] Bonanos N. *Preparation of Suzuki phases and their stability*", Materials Research Bulletin, 14, 12, 1609-1615, 1979

[21] B. Cornils *Aqueous-Phase Organometallic Catalysis: Concepts and Applications*, Wiley, Weinheim, New York, 2004.

[22] E.C. Sherer *Electronic structure and bonding in hexacoordinate silyl–palladium complexes*, Angew. Chem. Int. Ed. 41 1953, (2002)

[23] T. Mizoroki *Arylation of olefin with aryl iodide catalyzed by palladium*, Bull. Chem. Soc. Jpn. 44 (1971) 581.

[24] Jun-ichi Yoshida *Continuous flow synthesis*, Drug Discovery Today: Technologies, Vol.10, 2013

[25] D. Painer, M. Siebenhofer, *Reaktionstechnik II*, Skriptum, 2016

[26] Kiwi-Minsker *Microstructured reactors for catalytic reactions*, Catal. Today 110, 2–14, 2005

[27] Frost C.G. *Heterogeneous catalytic synthesis using microreactor technology*, Green Chem. 12, 1687–1703, 2010

[28] Kobayashi, J. et al. *Multiphase organic synthesis in microchannel reactors*, Chem. Asian J. 1, 22–35, 2006

[30] P. Prandner, *Residence –Time -Distribution of a Continuous Blender*, Construction exercise, 2016

[31] H.S. Ramaswamy *Residence time distribution (RTD) in aseptic processing of particulate foods: a review*", Food Research interenational, Vol. 28, No. 3, 291-303, 1995

[32] M. Lukasch *Synthese von Acetylsalicylsäure in einem Festbettreaktor*, Bachelor thesis, 2014

[33] Pichler Raphael *Modelling of a Continuous Catalytic Flow reactor*, Master thesis, 2015

[34] Robert L. Paddock *Co(III) porphyrin/DMAP: An Efficient Catalyst System for the Synthesis of Cyclic Carbonates from CO2 and Epoxides*, Tetrahedron Letters, 45(9): 3023-2026, 2004

[35] Tambar, U. K. (2003, April 17). The Heck Reaction:Mechanistic Insight into a Synthetically Useful Reaction. *Stoltz Group Literature Series.*

[36] Walter Carbi, Recent Developments and New Perspectives in the Heck Reaction, Acc. Chem. Res. 1995, 28, 2-7

[37] Internet: Catalysis Heck-reaction: https://chem.libretexts.org/Core/Inorganic_Chemistry/Catalysis/Catalyst_Examples/Heck_Reaction (visited on 30.04.2018)

[38] Internet: Suzuki-reaction: http://hwpi.harvard.edu/files/myers/files/12-the_suzuki_reaction.pdf (visited on 30.04.2018)

[39] Baumann, M. et al. *The flow synthesis of heterocycles for natural product and medicinal chemistry applications*, Mol. Divers. 15, 613–630, 2011

[40] Internet: residence time distribution: https://coanda.ca/blog/residence-time-distribution-measurements/ (visited on 30.04.2018)

[41] “New continuous tumble mixer characterization”, Miguel Florian, Carlos Velazquez Rafael Mendez, Puerto Rico 2014

[42] Sebastion Kozuch *“Turning Over” Definitions in Catalytic Cycles,* ACS Catalysis, American Chemical Society, 2012, 2, 2787-2794

Appendix

Appendix A Particle Analysis

BET surface analysis of the granulate

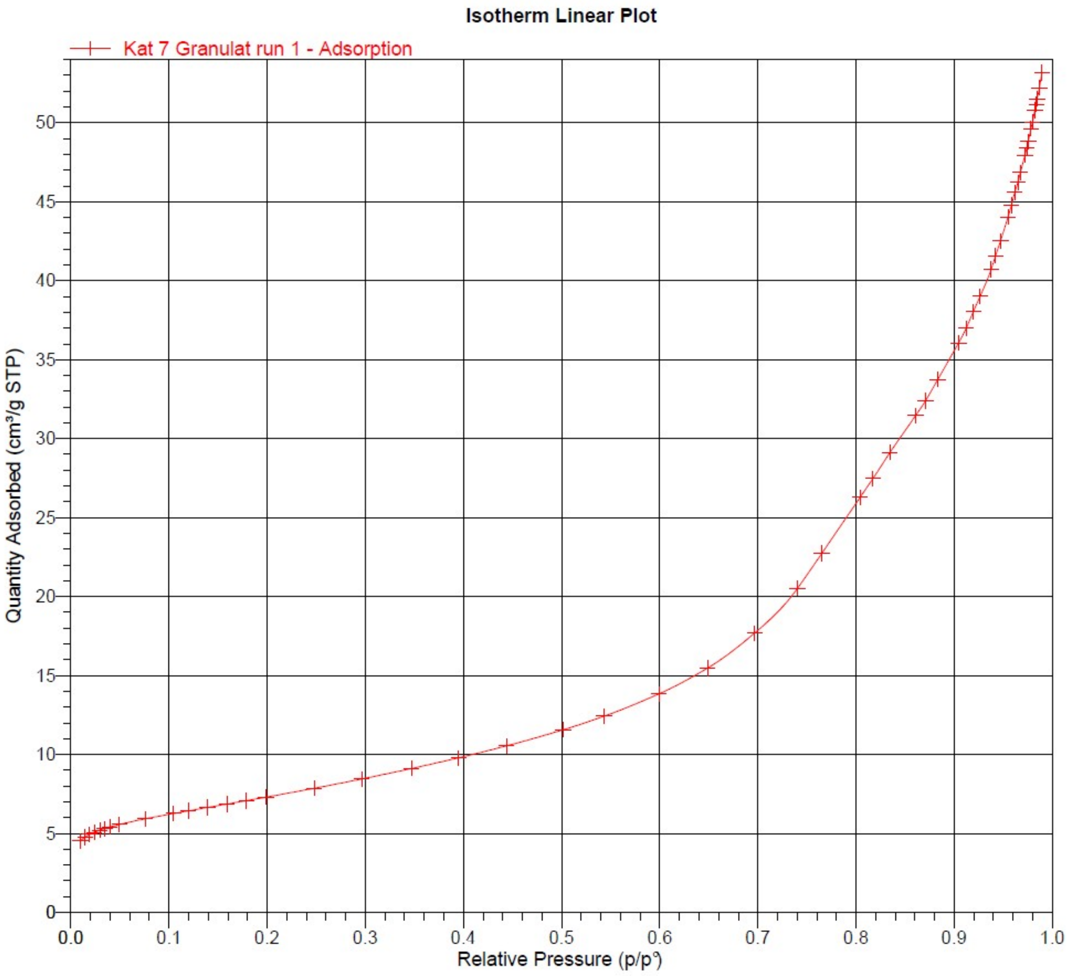

BET Surface Area Report

BET Surface Area: 26.1828 ± 0.1048 m²/g
Slope: 0.164935 ± 0.000659 g/cm³ STP
Y-Intercept: 0.001326 ± 0.000090 g/cm³ STP
C: 125.339597
Qm: 6.0146 cm³/g STP
Correlation Coefficient: 0.9999521
Molecular Cross-Sectional Area: 0.1620 nm²

Relative Pressure (p/p°)	Quantity Adsorbed (cm³/g STP)	$1/[Q(p^\circ/p - 1)]$
0.049542767	5.5675	0.009362
0.075517632	5.9201	0.013798
0.104701783	6.2617	0.018676
0.119590091	6.4275	0.021133
0.139105437	6.6402	0.024334
0.158863357	6.8547	0.027553
0.178871703	7.0737	0.030795
0.198708761	7.2933	0.034002

BET-adsorption isotherm for catalyst

QICPIC results of granulate before it was used in a reaction:

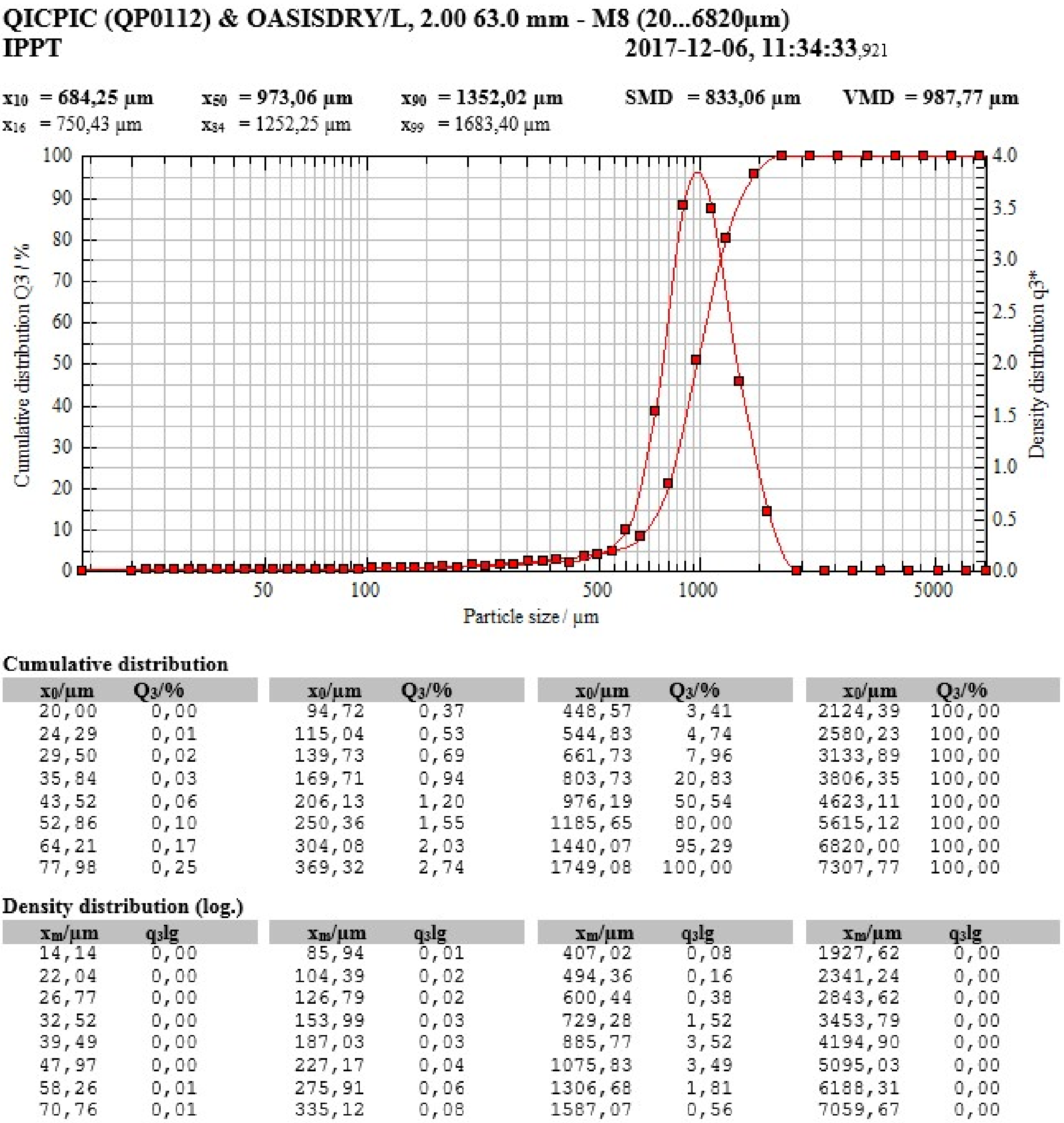

QICPIC (QP0112) & OASISDRY/L, 2.00 63.0 mm - M8 (20...6820µm)
IPPT 2017-12-06, 11:34:33,921

x_{10} = 684,25 µm **x_{50} = 973,06 µm** **x_{90} = 1352,02 µm** **SMD = 833,06 µm** **VMD = 987,77 µm**
x_{16} = 750,43 µm x_{84} = 1252,25 µm x_{99} = 1683,40 µm

Cumulative distribution

x_0/µm	Q_3/%	x_0/µm	Q_3/%	x_0/µm	Q_3/%	x_0/µm	Q_3/%
20,00	0,00	94,72	0,37	448,57	3,41	2124,39	100,00
24,29	0,01	115,04	0,53	544,83	4,74	2580,23	100,00
29,50	0,02	139,73	0,69	661,73	7,96	3133,89	100,00
35,84	0,03	169,71	0,94	803,73	20,83	3806,35	100,00
43,52	0,06	206,13	1,20	976,19	50,54	4623,11	100,00
52,86	0,10	250,36	1,55	1185,65	80,00	5615,12	100,00
64,21	0,17	304,08	2,03	1440,07	95,29	6820,00	100,00
77,98	0,25	369,32	2,74	1749,08	100,00	7307,77	100,00

Density distribution (log.)

x_m/µm	$q_3$lg	x_m/µm	$q_3$lg	x_m/µm	$q_3$lg	x_m/µm	$q_3$lg
14,14	0,00	85,94	0,01	407,02	0,08	1927,62	0,00
22,04	0,00	104,39	0,02	494,36	0,16	2341,24	0,00
26,77	0,00	126,79	0,02	600,44	0,38	2843,62	0,00
32,52	0,00	153,99	0,03	729,28	1,52	3453,79	0,00
39,49	0,00	187,03	0,03	885,77	3,52	4194,90	0,00
47,97	0,00	227,17	0,04	1075,83	3,49	5095,03	0,00
58,26	0,01	275,91	0,06	1306,68	1,81	6188,31	0,00
70,76	0,01	335,12	0,08	1587,07	0,56	7059,67	0,00

QICPIC results of granulate after it was used in a reaction:

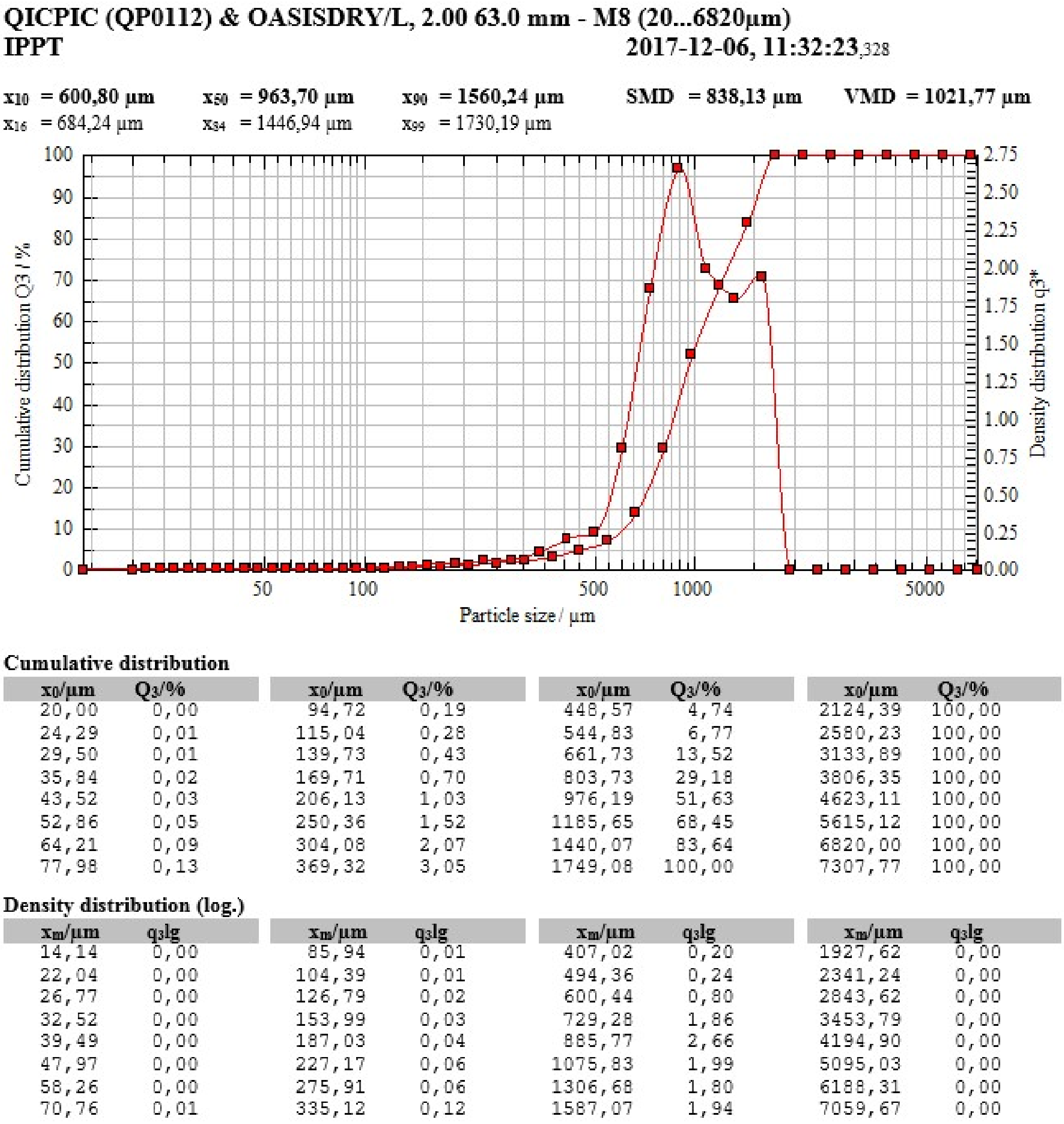

QICPIC (QP0112) & OASISDRY/L, 2.00 63.0 mm - M8 (20...6820µm)
IPPT **2017-12-06, 11:32:23**,328

x_{10} = 600,80 µm **x_{50} = 963,70 µm** **x_{90} = 1560,24 µm** **SMD = 838,13 µm** **VMD = 1021,77 µm**
x_{16} = 684,24 µm x_{84} = 1446,94 µm x_{99} = 1730,19 µm

Cumulative distribution

x_0/µm	Q_3/%	x_0/µm	Q_3/%	x_0/µm	Q_3/%	x_0/µm	Q_3/%
20,00	0,00	94,72	0,19	448,57	4,74	2124,39	100,00
24,29	0,01	115,04	0,28	544,83	6,77	2580,23	100,00
29,50	0,01	139,73	0,43	661,73	13,52	3133,89	100,00
35,84	0,02	169,71	0,70	803,73	29,18	3806,35	100,00
43,52	0,03	206,13	1,03	976,19	51,63	4623,11	100,00
52,86	0,05	250,36	1,52	1185,65	68,45	5615,12	100,00
64,21	0,09	304,08	2,07	1440,07	83,64	6820,00	100,00
77,98	0,13	369,32	3,05	1749,08	100,00	7307,77	100,00

Density distribution (log.)

x_m/µm	$q_3$lg	x_m/µm	$q_3$lg	x_m/µm	$q_3$lg	x_m/µm	$q_3$lg
14,14	0,00	85,94	0,01	407,02	0,20	1927,62	0,00
22,04	0,00	104,39	0,01	494,36	0,24	2341,24	0,00
26,77	0,00	126,79	0,02	600,44	0,80	2843,62	0,00
32,52	0,00	153,99	0,03	729,28	1,86	3453,79	0,00
39,49	0,00	187,03	0,04	885,77	2,66	4194,90	0,00
47,97	0,00	227,17	0,06	1075,83	1,99	5095,03	0,00
58,26	0,00	275,91	0,06	1306,68	1,80	6188,31	0,00
70,76	0,01	335,12	0,12	1587,07	1,94	7059,67	0,00

Wavelengths of quantification and retention times for the used internal standards, substrates and the observed products

	Retention time t_r [min]	Wave length of quantification [nm]
Internal standard		
Anisole	4.34	237
Substrates		
Phenylboronic acid	1.31	237
4-Bromotoluene	9.5	237
Iodobenzene	8.7	237
3-Butene-2ol	not visible (not UV-active)	
Products		
4-Methylbiphenyl	11.12	237
4-Phenyl-but-3-en2-ol	5.2	237

Appendix B Calibration

Calibration of investigated chemicals at HPLC for a wavelength of 237 nm.

Suzuki-reaction:

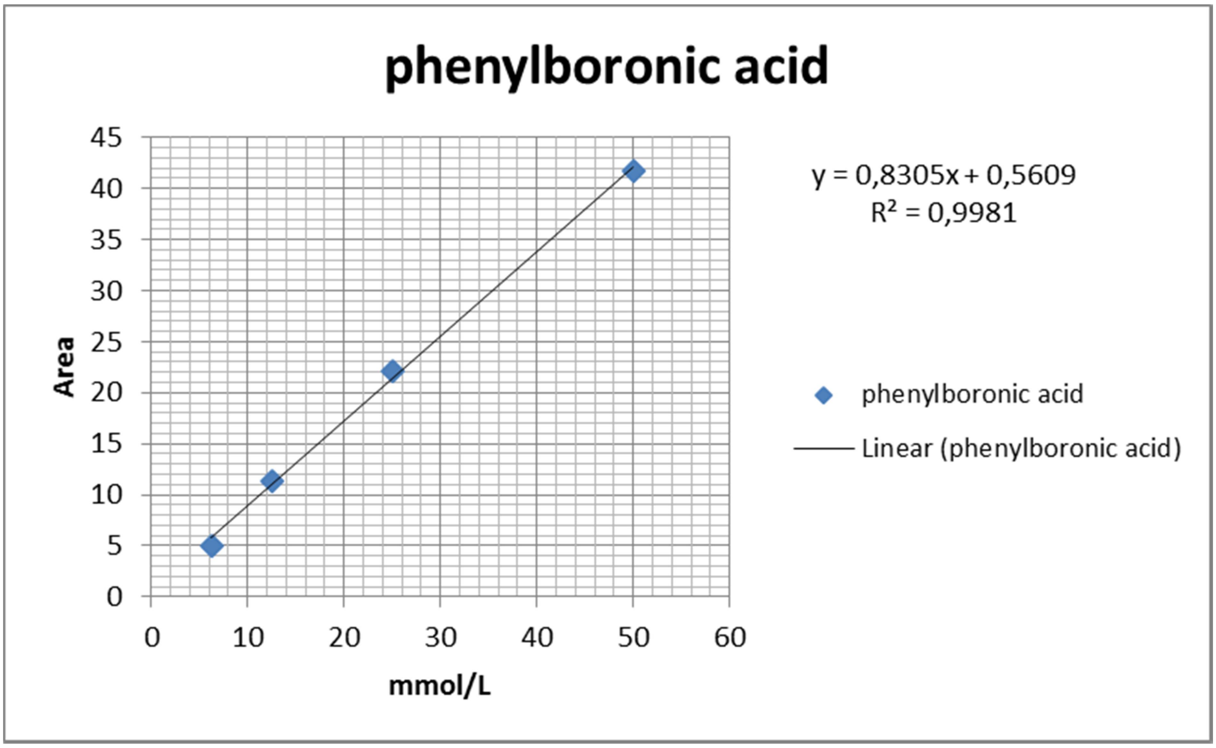

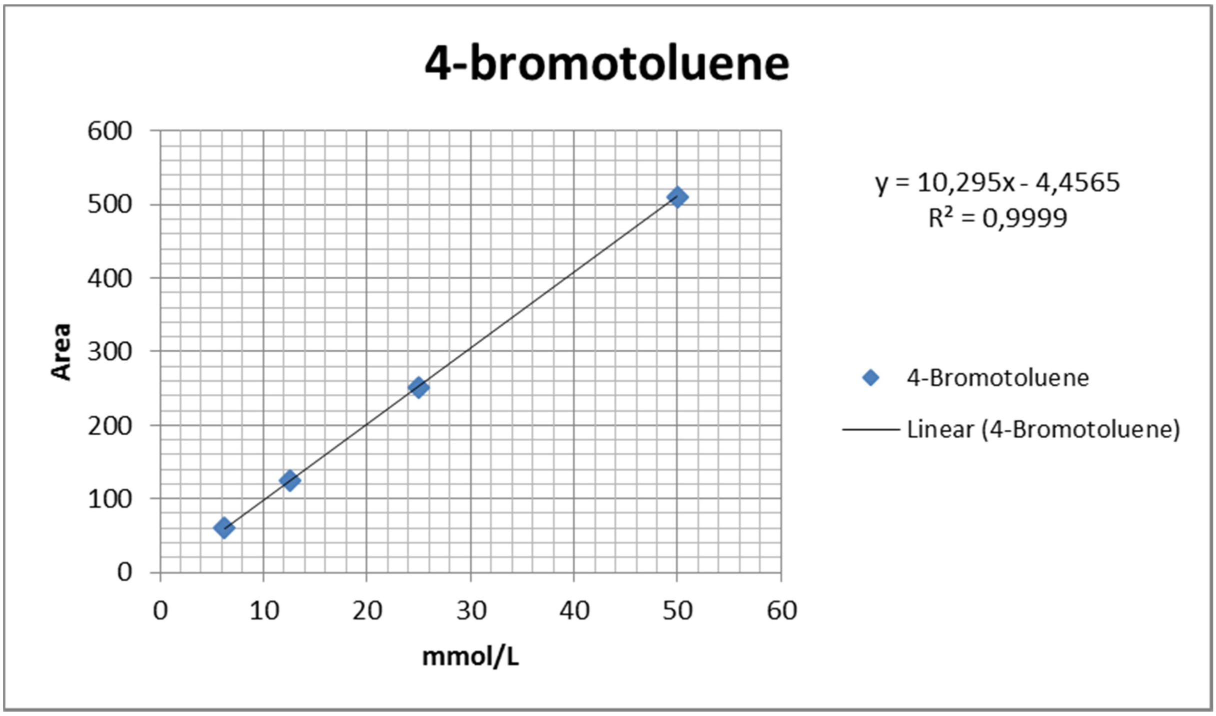

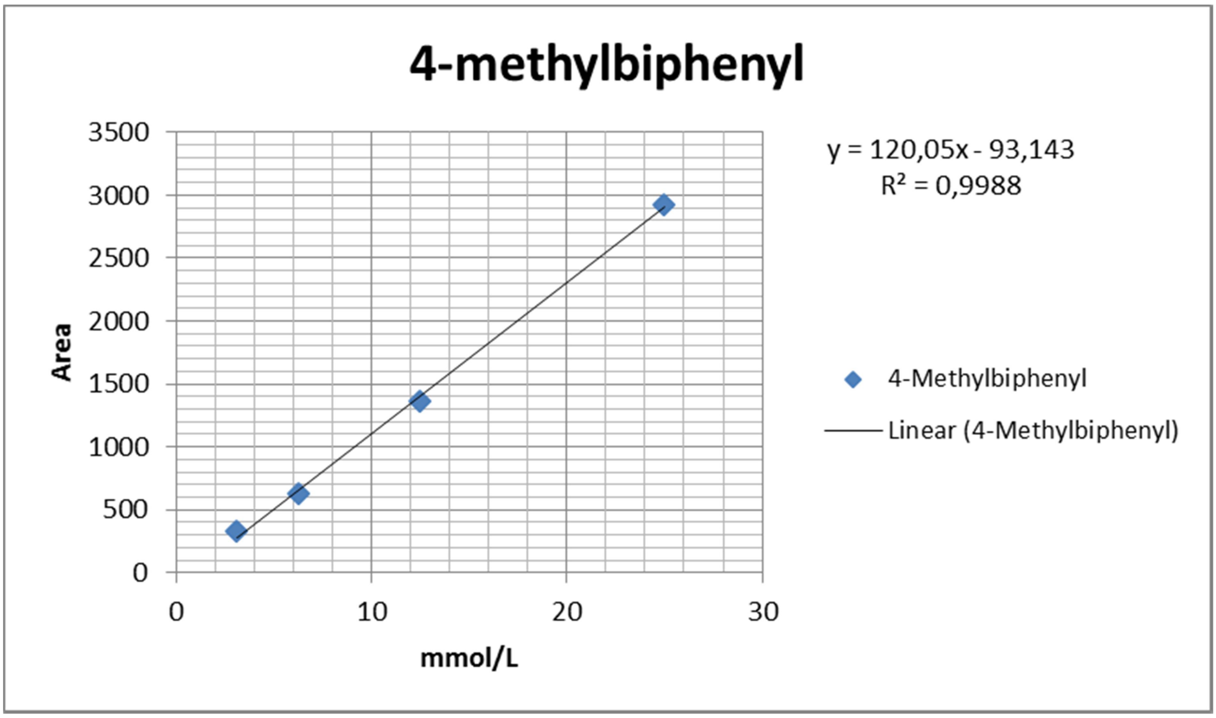

Heck-reaction:

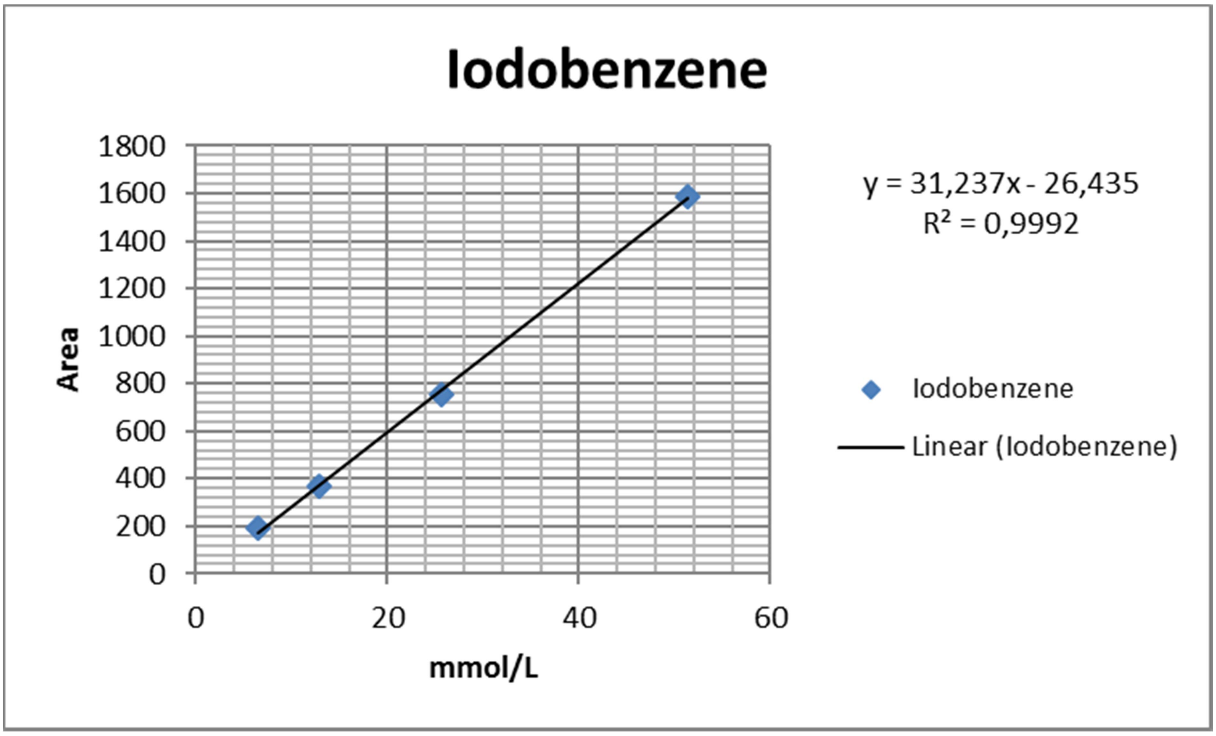

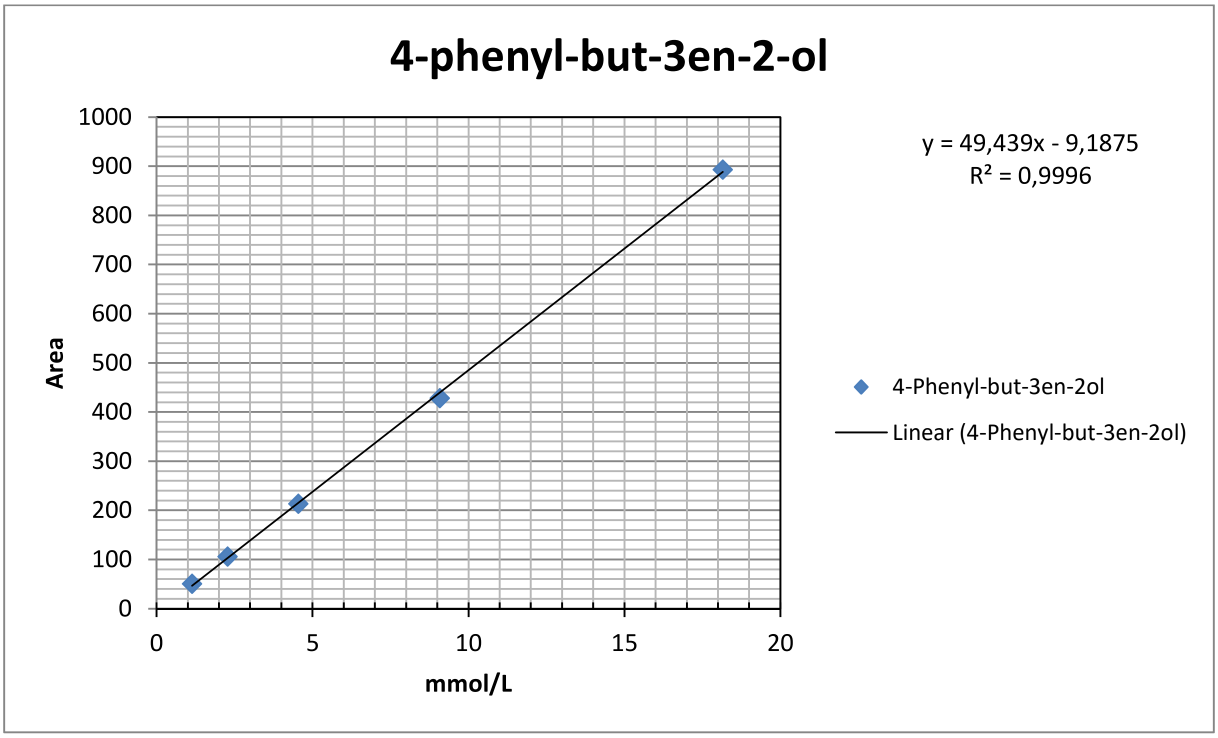
4-phenyl-but-3en-2-ol
y = 49,439x - 9,1875
R² = 0,9996
Area
1000
900
800
700
600
500
400
300
200
100
0
0
5
10
15
20
mmol/L
4-Phenyl-but-3en-2ol
Linear (4-Phenyl-but-3en-2ol)

Appendix C Results RTD

Columns: **2**
FlowRate: **0,5** **ml/min**

			$F(t)=\frac{c_{aus}}{c\_max}$	$t*\Delta c$	$t^2*\Delta c$	$E(t)=\frac{\Delta F(t)}{\Delta t}$	$E_\theta = E(t)*\bar{t}$	$F_\theta = F_{\theta,i\text{-}1}+E_\theta*\Delta\theta$	$\theta=\frac{t}{\bar{t}}$	$E_\theta*\theta$
Time	Area									
[min]	-	%	F(t)			E(t)	E(θ)	F(θ)	θ	
2	0	0	0	0	0	0	0	0	0.251	0
4	0	0	0	0	0	0	0	0	0.502	0
6	68.9	36.747	0.367	413.4	2480.4	0.184	1.463	0.367	0.754	1.102
8	145.6	77.653	0.777	613.6	4908.8	0.205	1.629	0.777	1.005	1.636
10	175.6	93.653	0.937	300	3000	0.08	0.637	0.937	1.256	0.8
12	181.5	96.8	0.968	70.8	849.6	0.016	0.125	0.968	1.507	0.189
14	184.5	98.4	0.984	42	588	0.008	0.064	0.984	1.758	0.112
16	185.2	98.773	0.988	11.2	179.2	0.002	0.015	0.988	2.009	0.030
18	187.3	99.893	0.999	37.8	680.4	0.0056	0.045	0.999	2.261	0.1008
20	187.4	99.947	0.999	2	40	0.0003	0.002	0.999	2.512	0.0053
22	187.5	100	1	2.2	48.4	0.0003	0.002	1	2.763	0.0059
c_max	187.5		Summe:	1493	12774.8					

$$\bar{t}=\frac{\sum t*\Delta c}{c_{max}}$$ 7.9627 min wenn:

		Bo > 100	Bo < 100
σ(t)²	4.7282	26.82	30.35
σ(θ)²	0.0746		

Columns: **2**
FlowRate **0,45** **ml/min**

Time [min]	Area -	%	$F(t)=\frac{c_{aus}}{c\_max}$ F(t)	$t*\Delta c$	$t^2*\Delta c$	$E(t)=\frac{\Delta F(t)}{\Delta t}$ E(t)	$E_\theta = E(t)*\bar{t}$ E(θ)	$F_\theta = F_{\theta,i\text{-}1}+E_\theta*\Delta\theta$ F(θ)	$\theta=\frac{t}{\bar{t}}$ θ	$E_\theta*\theta$
2	0	0	0	0	0	0	0	0	0.236	0
4	0	0	0	0	0	0	0	0	0.473	0
6	57	29.86	0.2986	342	2052	0.149	1.263	0.299	0.709	0.896
8	138.2	72.39	0.7239	649.6	5196.8	0.213	1.799	0.724	0.946	1.701
10	169	88.53	0.8853	308	3080	0.081	0.683	0.885	1.182	0.807
12	181.6	95.13	0.9513	151.2	1814.4	0.033	0.279	0.951	1.418	0.396
14	183.9	96.33	0.9633	32.2	450.8	0.006	0.051	0.963	1.655	0.084
16	184.7	96.75	0.9675	12.8	204.8	0.002	0.018	0.968	1.891	0.034
18	189.7	99.37	0.9937	90	1620	0.013	0.111	0.994	2.127	0.236
20	189.4	99.21	0.9921	-6	-120	-0.001	-0.007	0.992	2.364	-0.016
22	190.2	99.63	0.9963	17.6	387.2	0.002	0.018	0.996	2.600	0.046
24	190.5	99.79	0.9979	7.2	172.8	0.001	0.007	0.998	2.837	0.019
26	190.8	99.95	0.9995	7.8	202.8	0.001	0.007	0.999	3.073	0.020
28	190.9	100	1	2.8	78.4	0.000	0.002	1	3.309	0.007
30	190.9	100	1	0	0	0	0	1	3.546	0
c_max:	190.9		summe:	1615.2	15140					

$\bar{t}=\frac{\sum t*\Delta c}{c_{max}}$ 8.4609 min

wenn:

		Bo > 100	Bo < 100
σ(t)²	7.7204	18.545	21.9279
σ(θ)²	0.1078		

Columns: **3**

FlowRate **0,45** **ml/min**

Time [min]	Area -	%	$F(t) = \frac{c_{aus}}{c\_max}$ F(t)	$t * \Delta c$	$t^2 * \Delta c$	$E(t) = \frac{\Delta F(t)}{\Delta t}$ E(t)	$E_\theta = E(t) * \bar{t}$ E(θ)	$F_\theta = F_{\theta,i\text{-}1} + E_\theta * \Delta\theta$ F(θ)	$\theta = \frac{t}{\bar{t}}$ θ	$E_\theta * \theta$
2	0	0	0	0	0	0	0	0	0.1767	0
4	0	0	0	0	0	0	0	0	0.3533	0
6	0	0	0	0	0	0	0	0	0.5300	0
8	10.4	7.619	0.0761	83.2	665.6	0.0380	0.4312	0.0761	0.7066	0.3047
10	78.9	57.802	0.5780	685	6850	0.2509	2.8407	0.5780	0.8833	2.5091
12	107.1	78.461	0.7846	338.4	4060.8	0.1032	1.1694	0.7846	1.0599	1.2395
14	122.9	90.036	0.9003	221.2	3096.8	0.0578	0.6552	0.9003	1.2366	0.8102
16	136.5	100	1	217.6	3481.6	0.0498	0.5640	1	1.4132	0.7970
18	136.5	100	1	0	0	0	0	1	1.5899	0
20	136.5	100	1	0	0	0	0	1	1.7665	0
22	136.5	100	1	0	0	0	0	1	1.9432	0
24	136.5	100	1	0	0	0	0	1	2.1198	0
26	136.5	100	1	0	0	0	0	1	2.2965	0
28	136.5	100	1	0	0	0	0	1	2.4731	0
30	136.5	100	1	0	0	0	0	1	2.6498	0
c_max:	136.5		summe:	1545.4	18154.8					

$\bar{t} = \frac{\sum t * \Delta c}{c_{max}}$ 11.321 min

		wenn:	
		Bo > 100	Bo < 100
σ(t)²	4.8233	53.149	56.887
σ(θ)²	0.0376		

Columns: **1**
FlowRate **0,45** **ml/min**

Time [min]	Area -	 %	$F(t) = \frac{c_{aus}}{c\_max}$ F(t)	$t * \Delta c$	$t^2 * \Delta c$	$E(t) = \frac{\Delta F(t)}{\Delta t}$ E(t)	$E_\theta = E(t) * \bar{t}$ E(θ)	$F_\theta = F_{\theta,i\text{-}1} + E_\theta * \Delta\theta$ F(θ)	$\theta = \frac{t}{\bar{t}}$ θ	$E_\theta * \theta$
2	0	0	0	0	0	0	0	0	0.2748	0
4	7.2	5.2747	0.0527	28.8	115.2	0.0263	0.1919	0.0527	0.5496	0.1054
6	95.4	69.8901	0.6989	529.2	3175.2	0.3230	2.3512	0.6989	0.8244	1.9384
8	116.1	85.0549	0.8505	165.6	1324.8	0.0758	0.5518	0.8505	1.0993	0.6065
10	121.6	89.0842	0.8908	55	550	0.0201	0.1466	0.8908	1.3741	0.2014
12	126.2	92.4542	0.9245	55.2	662.4	0.01684	0.1226	0.9245	1.6489	0.2021
14	132.4	96.9963	0.9699	86.8	1215.2	0.02271	0.1652	0.9699	1.9237	0.3179
16	133.8	98.0219	0.9802	22.4	358.4	0.00512	0.0373	0.9802	2.1985	0.0820
18	135.6	99.3406	0.9934	32.4	583.2	0.00659	0.0479	0.9934	2.4733	0.1186
20	136.5	100	1	18	360	0.00329	0.0239	1	2.7481	0.0659
22	136.5	100	1	0	0	0	0	1	3.0230	0
24	136.5	100	1	0	0	0	0	1	3.2978	0
26	136.5	100	1	0	0	0	0	1	3.5726	0
28	136.5	100	1	0	0	0	0	1	3.8474	0
30	136.5	100	1	0	0	0	0	1	4.1222	0
c_max:	136.5		summe:	993.4	8344.4					

$\bar{t} = \frac{\sum t * \Delta c}{c_{max}}$	7.277	min	wenn:	
			Bo > 100	Bo < 100
σ(t)²	8.166		12.9705	16.1775
σ(θ)²	0.154			